EML 4905 Senior Design Project

A B.S. THESIS
PREPARED IN PARTIAL FULFILLMENT OF THE
REQUIREMENT FOR THE DEGREE OF
BACHELOR OF SCIENCE
IN
MECHANICAL ENGINEERING

HySol
Integrated Solid Hybrid Rocket Booster
100 % Report

Dennis Moreno
Eduardo Gorrochotegui
Pedro Serrat

Advisor: Dr. Igor Tsukanov

April 9, 2013

This B.S. thesis is written in partial fulfillment of the requirements in EML 4905. The contents represent the opinion of the authors and not the Department of Mechanical and Materials Engineering.

Ethics Statement and Signatures

The work submitted in this B.S. thesis is solely prepared by a team consisting of Dennis Moreno, Eduardo Gorrochotegui, Pedro Serrat and it is original. Excerpts from others' work have been clearly identified, their work acknowledged within the text and listed in the list of references. All of the engineering drawings, computer programs, formulations, design work, prototype development and testing reported in this document are also original and prepared by the same team of students.

Dennis Moreno	Eduardo Gorrochotegui	Pedro Serrat
Team Leader	Team Member	Team Member

Dr. Igor Tsukanov

Faculty Advisor

Abstract

This thesis addresses the development of a valve system, which would properly integrate a solid and a hybrid rocket motor. The challenge provided to team HySol by Environmental Aeroscience Corporation (eAc) was to develop a rocket that would reach the current amateur altitude limit of 90 miles.

Two types of rocket systems were integrated in the design, in order to achieve the desired altitude. A solid rocket system was used in the first stage, and later transitioned into a hybrid rocket system. The solid rocket segment provided a short burst of high thrust, while the hybrid rocket stage provided low thrust for a prolonged period of time. In order to combine two different rocket systems efficiently, a multiple valve system was designed and integrated in the core of the rocket motor. The valves atomize the oxidizer in the hybrid system, which burns the fuel in the second stage of the rocket. Without proper development and implementation of the valve, the rocket would not effectively transition from one power source to another. If the oxidizer were released prior to the optimal transition point, the time of thrust supplied would be minimized. The opposing situation where the oxidizer is released after the optimal transition point would also hinder the overall performance of the system. The thrust of the rocket motor would reduce prior to ignition of the hybrid stage and a smooth transition of the system would not be achieved. The rocket would lose some altitude gained by the initial given thrust before releasing the second stage hybrid motor. The proper design of the valve system, alongside optimal integration, allowed the team to achieve the overall goals anticipated by eAc.

Acknowledgments

The team would like to thank Environmental Aeroscience Corporation and Syntheon for supporting the HySol project. We are especially grateful to Korey Klein and Derek Deville for their contribution of advice and technical expertise. The team would also like to thank Kevin Smith and Tom Bales for allowing us to use their state of the art manufacturing facility. Also, Max Mendez was instrumental to the setup of the data acquisition system. We would like to thank Jorge Pinos and Angel Fernandez for their willingness to assist us with the machine work. Finally, the team would like to thank our families for their support and patience throughout the duration of the project.

Table of Contents

List of Figures

List of Tables

1. Introduction

1.1. Problem Statement

In December 2008, the United States Government increased the limitations for Amateur Rockets. Originally set under 80 miles, the current law allows Amateur Rockets to fly up to an altitude of 93 miles (Register). The challenge faced was to have enough thrust for initial lift off and rise, as well as enough fuel to continue towards the altitude goal of 93 miles.

Environmental Aeroscience Corporation had the desire to surpass the current Amateur Rocket altitude record. The problem faced was the ability to combine two different rocket motors and have them efficiently provide thrust throughout its flight. In order to achieve the goals, a valve system for an integrated solid hybrid rocket motor had to be designed.

The customer indicated the need to design a simple transition system to minimize possible failure while having a low cost. The system would allow a smooth transition from a solid to a hybrid propellant stage by releasing an oxidizer (N_2O) at the optimal time. The solid and the hybrid stages, integrated by the valve system, would need to be tested individually to find the optimal point of transition. If done properly, the rocket would encounter minimal resistance when transitioned into the prolonged hybrid stage.

1.2. Motivation

To be industry pioneers within a field where minimum information was readily available can prove to be quite difficult. The greatest motivation behind this project was to surpass the current amateur rocket altitude record by reaching the current limit of 93 miles (Hobby Space). Becoming industry pioneers proved to be challenging, yet motivating. Extensive research was

done in order to learn more about the combination of two rocket technologies, which have not been used together before. In doing so, we were able to open the door for the beginning steps of research and standards, as well as pave the way for further research in similar topics. Alongside the research needed to develop the new technology and launch the rocket, the team wrote a technical paper, which will be submitted to the American Institute of Aeronautics and Astronautics (AIAA). This will provide proper documentation of the research and findings done, as well as provide easy access to information for future rocketeers.

1.3. Literature Survey

Theodore Levitt an American Economist and professor at Harvard Business School once said, “Creativity is thinking up new things. Innovation is doing new things.” The first successful spaceflight was in 1957 when the Soviet Union launched the world’s first satellite, Sputnik 1, into orbit. It was this event that sparked the space race with the United States. It would be 11 years later when the first man in space was accomplished again by the Soviet Union in 1961 by Yuri Gagarin (Shepherd). However, on July 20, 1969 the United States became truly innovative and landed the first humans on the moon. Launched by a Saturn V rocket on July 16th it would be the fifth manned mission from NASA’s Apollo Program (Cadbury, 2006).

With the launch of Sputnik, the private sector became fascinated with rocketry; even though the history of amateur rocketry dates back to the 1930’s, this event was the momentum needed to get the hobby in full effect. One of the first US organizations to be involved in amateur rocketry was Pacific Rocket Society, which was formed in California in the early 1950’s and is still in existence today. It was in 1988 when The Space Frontier Foundation was formed, the foundation consisted of a group of space community leaders with the vision to expand rocketry research and the advancement of technology in order to achieve a lower cost for space

access. In November 1997, the Space Frontier Foundation and the Foundation for the International Non-governmental Development of Space (FINDS) jointly announced a $250,000 prize for the first private team to launch a 2 kilogram payload into space, 124 miles or higher, by November 8, 2000, using a privately developed launcher as specified within the rules. Called the CATS Prize, The Foundation and FINDS wanted to show that space was not purely the domain of governments. Alas, November 8th came and went and no company or individual was able to claim success (Muncy). Started just one year before Space Frontier Foundation; Dr. Peter Diamandis designed the X prize modeled after the Orteig Prize. Reading the spirit of St. Louis a story about the winning of the Orteig Prize inspired Dr. Diamandis. The Prize would award $10 million dollars to the team that could launch a spacecraft capable of transporting three people to 100 km above the earth's surface, twice within two weeks. It would be on October 4, 2004 (47 years after the Soviet Union launched Sputnik 1) where prestigious aerospace designer Burt Rutan of Scaled Composites would pioneer a new industry with his SpaceShipOne and win the X PRIZE. This was accomplished by using a hybrid rocket booster for the propulsion system on the spacecraft (2nd Stage) the hybrid rocket would produce 10,000lbs of thrust for one minute. With the award of the prize would bring new technologies that would allow space tourism and the deployment of satellites into low earth orbits more feasible and cost effective.

Figure 1: SpaceShipOne Rocket testing (eAc)

1.4. Background

Solid rocket motors use solid fuel to provide thrust to the system. There are two types of propellant grains that can be used in these motors: homogeneous and composite propellants. In homogeneous systems, the fuel and oxidizer are confined inside the same molecule and then they decompose during the combustion process. Nitroglycerine and Nitrocellulose are some examples of homogeneous rocket propellant. Heterogeneous systems are composed of a mixture of oxidizing crystals in a polymer binder that acts as fuel. Metal powders can also be added to the mixture to increase the energy of the combustion process and also the density of the fuel.

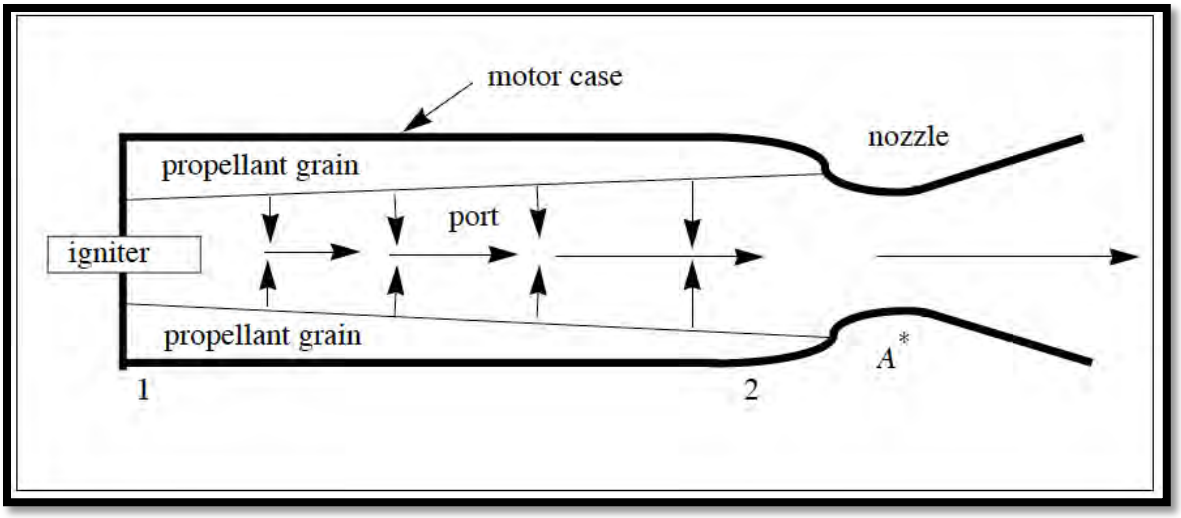

Figure 2: Solid Rocket Motor

Hybrid rocket motors use propellants in two different states of matter to provide thrust to the system. The oxidizer, usually liquid or gas burns with a solid fuel. Hybrid rockets have several advantages over solid rockets in different fields. They are naturally safer to operate since the oxidizer and fuel are not immediately mixed in the event of a system failure. Unlike solid rockets, they can be throttled and shut down easily.

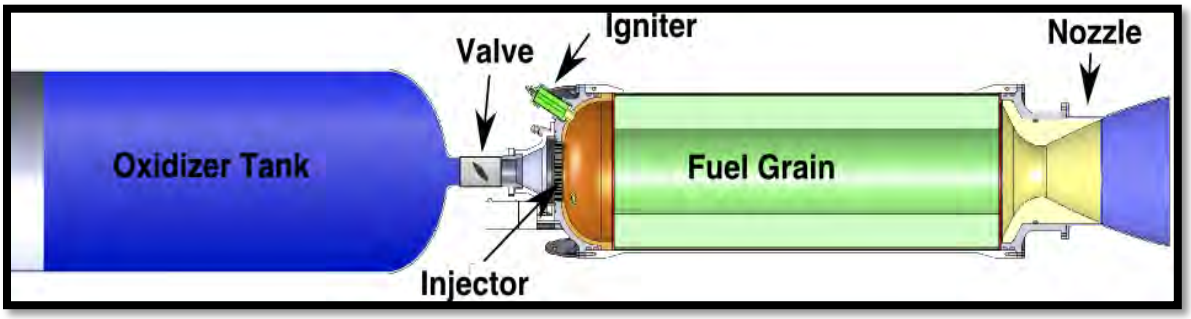

Figure 3: Hybrid Rocket Motor (Cantwell D. B.)

2. Design

2.1. Concept 1:

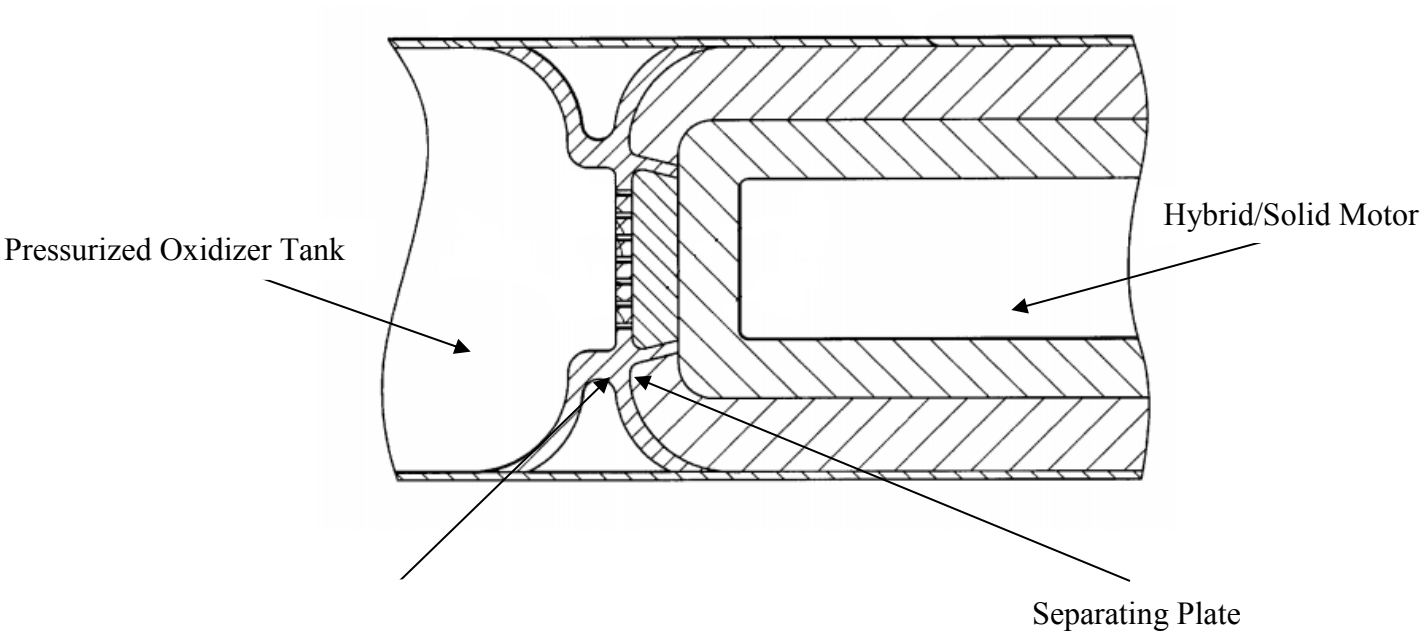

Figure 4: Concept 1 (Kline, 1998)

This design calls for a multi-tube valve system that is placed between the oxidizer tank and the hybrid/solid motor. The multi-tube valve is sealed by a separating plate which is manufactured of low melting temperature metal. The plate assists in withstanding the increase in pressure once ignited, and prevents the oxidizer from entering the motor early. Once the solid propellant regresses to the metal plate, the increased temperature will melt the plate and open the multi-tube valve system and commence the second stage into the hybrid motor. A multi-tube valve system will allow a well-distributed flow of oxidizer, as well as an increase in atomization.

2.2. Concept 2:

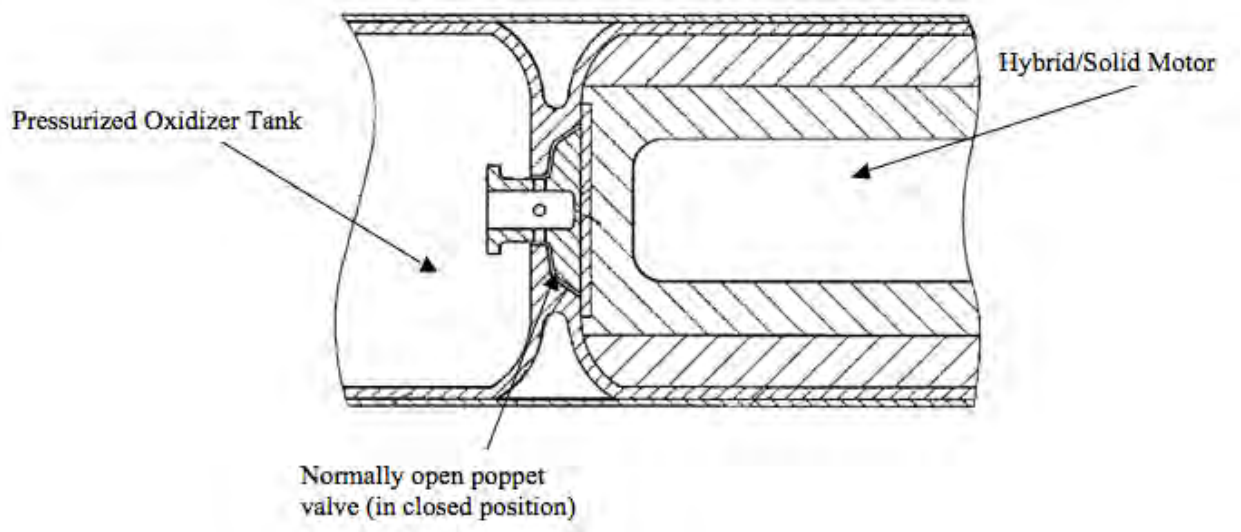

Figure 5: Concept 2 (Kline, 1998)

This design calls for a poppet valve that is normally open. During manufacturing of the motor the poppet valve will be mechanically closed additionally the solid propellant will aid the valve closure from the self-pressurizing oxidizer, which in this case is N_2O. During operation of the solid motor the chamber pressure will also aid in keeping the valve closed. Once the solid propellant has regressed additionally with the high temperature the poppet valve will open and commence the hybrid motor, the secondary stage.

2.3. Concept 3:

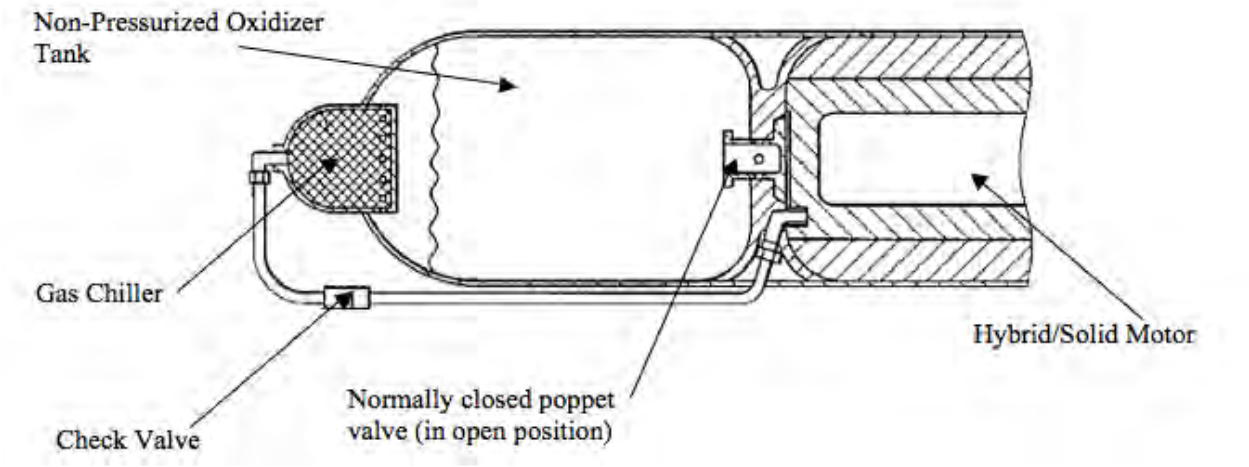

Figure 6: Concept 3 (Kline, 1998)

This design calls for a poppet valve that is normally closed. Alternatively, the oxidizer tank will not need to be pressurized. The solid propellant geometry will be configured in such a manner that the peak chamber pressure achieved during the end of the solid propellant burn thus providing a pressure source through the means of a check valve and a gas chiller to pressurize the oxidizer which will then open the valve and commence the hybrid motor, the secondary stage.

2.4. Concept 4:

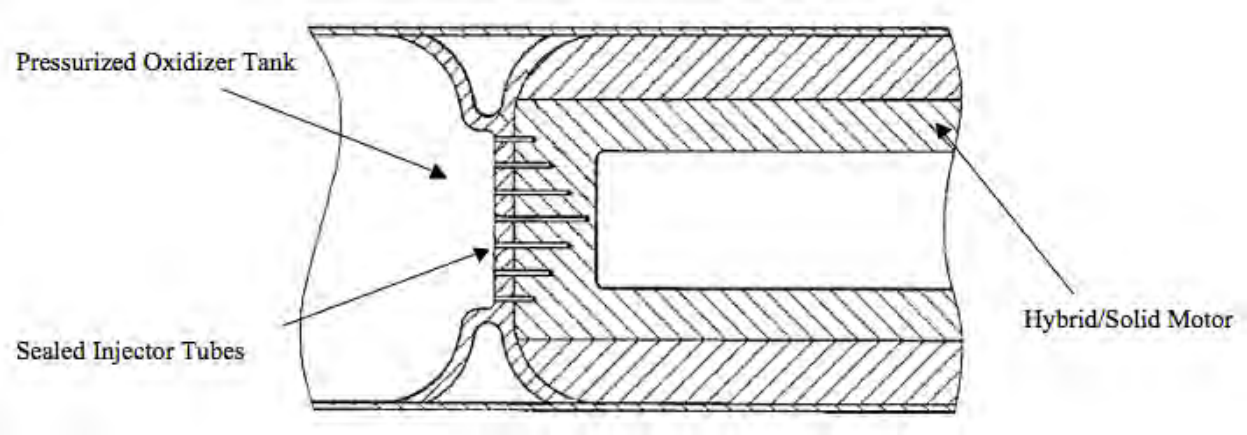

Figure 7: Concept 4 (Kline, 1998)

This design calls for an array of small injector tubes that are capped off with propellant or material with a predictable melting point closing from the self-pressurizing oxidizer, which in this case is N_2O. The solid propellant will burn and melt the propellant/material sealing the injector tubes and commence the hybrid motor, the secondary stage.

3. Proposed Design

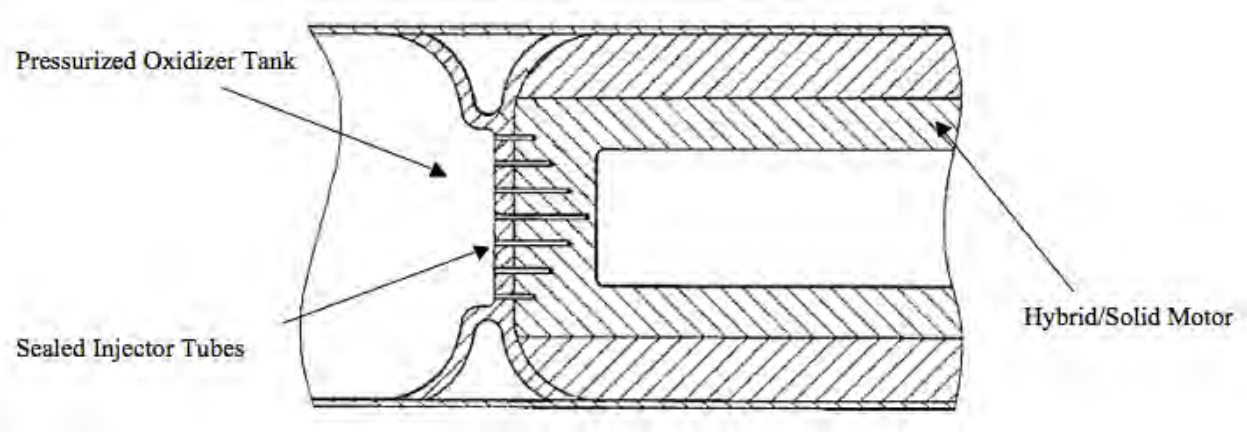

Figure 8: Proposed Design (Kline, 1998)

A high priority of the customer's input is to have a simple and low cost method to provide the switch from the solid motor to hybrid motor. In addition a minimum of 5 lbs/sec of oxidizer flow is need for small scale testing. After careful consideration and the use of a design flow chart, concept 4 was chosen. Using the solid propellant or predictable melting material to seal off the injector tubes will eliminate the need of any moving parts thus making it the most simplest and cost effective design. Additionally if the need of more oxidizer flow is need, more injector tubes can be added for quick iterations of the design if needed.

4. Project Management

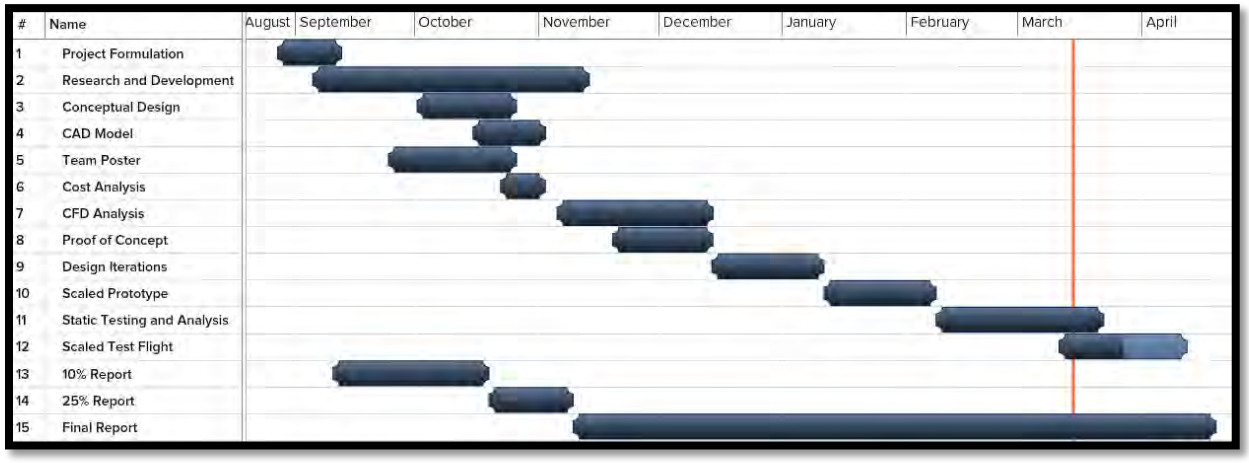

Figure 9: Gant chart

Table 1: Estimated hours needed

	Completed hours	Estimated hours needed
Dennis Moreno	385	400
Eduardo Gorrochotegui	385	400
Pedro Serrat	385	400

4.1. Responsibilities

Pedro Serrat:

- Subject matter expert of oxidizer (N_2O) characteristics
- Injector valve flow rates
- SolidWorks design.

Eduardo Gorrochotegui:

- Subject matter expert in heat transfer on injector system
- Injector valve flow rates
- SolidWorks design.

Dennis Moreno:

- Subject matter expert in propellant design
- Manufacturing expert
- Injector valve flow rates
- SolidWorks Design.

5. Engineering Design and Analysis

5.1. Analytical Analysis

A principal concern of this project is the method in which the motor will smoothly transition from a solid rocket booster to a hybrid rocket booster. In order to reach the desired altitude the motor will have to develop a minimum net total impulse of 115,000 lbs-s. This will be accomplished by using a novel rocket booster that is comprised of two stages; the first will be a high-pressure high thrust fast burn solid propellant grain. The second stage is a lower pressure, lower thrust, longer duration burn that will allow the rocket to continue to gain altitude running off the momentum of the first stage.

The total impulse of a rocket motor is how a rocket motor is classified and it is done so in letter designations. Ranging from "A" being the smallest to "X" being the largest, see Table 2 for motor specifications. Total Impulse can easily be calculated by the following equation:

$$\boldsymbol{I_t = W_f * I_{sp}} \qquad \textbf{(1)}$$

Where,

I_t = *Total Impulse*

W_f = *Total Fuel Weight*

I_{sp} = *Specific Impulse*

Table 2: Motor Classifications

Class	Total Impulse (Metric Standard)	Total Impulse (Imperial Standard)
A	1.26-2.50 N·s	0.29-0.56 lbf·s
B	2.51-5.00 N·s	0.57-1.12 lbf·s
C	5.01-10.00 N·s	1.13-2.24 lbf·s
D	10.01-20.00 N·s	2.25-4.48 lbf·s
E	20.01-40.00 N·s	4.49-8.96 lbf·s
F	40.01-80.00 N·s	8.97-17.92 lbf·s
G	80.01-160.00 N·s	17.93-35.96 lbf·s
H	160.01-320.00 N·s	35.97-71.92 lbf·s
I	320.01-640.00 N·s	71.93-143.83 lbf·s
J	640.01-1280.00 N·s	143.84-287.65 lbf·s
K	1,280.01-2,560.00 N·s	287.66-575.30 lbf·s
L	2,560.01-5,120.00 N·s	575.31-1150.60 lbf·s
M	5,120.01-10,240.00 N·s	1150.61-2301.20 lbf·s
N	10,240.01-20,480.00 N·s	2301.21-4602.40 lbf·s
O	20,480.01-40,960.00 N·s	4602.41-9204.80 lbf·s
P	40,960.01-81,920.00 N-s	9204.81-19409.60 lbf·s
Q	81,920.01-163,840.00 N-s	19409.61-38819.20 lbf·s
R	163,840.01-327,680.00 N-s	38819.21-77638.40 lbf·s
S	327,680.01-655,360.00 N-s	77638.41-155276.80 lbf·s
T	655,360.01-1,310,720.00 N-s	310553.81-621107.2 lbf·s
U	1,310,720.01-2,621,440.00 N-s	621107.21-1242214.40 lbf·s
V	2,621,440.01-5,242,880.00 N-s	1242214.41-2484428.80 lbf·s
W	5,242,880.01-10,485,760.00 N-s	2484428.81-4968857.60 lbf·s
X	10,485,760.01-20,971,520.00 N-s	4968857.60-9937715.2 lbf·s

In rockets, due to atmospheric effects, the specific impulse varies with altitude, reaching a maximum in a vacuum. This is because the exhaust velocity isn't simply a function of the chamber pressure, but is a function of the difference between the interior and exterior of the combustion chamber. It is therefore important to note if the specific impulse is vacuum or lower sea level. Values are usually indicated with or near the units of specific impulse

Rockets efficiency is measure by its specific impulse (I_{sp}). Specific Impulse can be generalized as the ratio of the thrust produced to the weight flow of the propellants expelled. Rocket motors are defined as jet motors that use stored propellant as means of propulsion. The motor designed is a two-stage rocket, consisting of a solid motor within a hybrid motor. During the first stage, combustion takes place in the inner most layers of the fuel grain, where the solid fuel and oxidizer mix is located. Once this layer is burned off, combustion will continue to the

hybrid fuel. At this point, a tank containing oxidizer releases the substance into the chamber, allowing for combustion to continue.

Specific Impulse (I_{sp}) is a ratio between the momentum and mass flow of the rocket. In order words, it measures the thrust accumulated as fuel is consumed, thrust is the force that propels the rocket though the air. Thrust is generated by the reaction of accelerating a gas out the nozzle. Ideally one would like to have this gas with as much mass as possible. Using Newton's second law of motions, force is defined as the change in momentum of an object. Momentum is simply the mass of an object multiplied by its velocity, thus when dealing with gas the thrust equation is as follows:

$$F = \dot{m}_e V_e - \dot{m}_o V_o + (P_e - P_o) A_e \qquad \textbf{(2)}$$

Where:

$F\ is\ the\ thrust$

$\dot{m}_e\ is\ the\ mass\ flow\ rate\ exiting$

$V_e\ is\ the\ velocity\ of\ the\ gass\ exiting$

$\dot{m}_o\ is\ the\ mass\ flow\ rate\ of\ the\ free\ stream$

$V_o\ is\ the\ velocity\ of\ the\ free\ stream$

$(P_e - P_o)\ is\ the\ pressure\ difference\ between\ the\ chamber\ and\ ambient\ pressure$

$A_e\ is\ the\ cross\ sectional\ area\ of\ the\ throat\ of\ the\ nozzel$

In the case of a rocket motor there is no free stream air taken into account thus the thrust equation simplifies to:

$$F = \dot{m}_e V_e + (P_e - P_o) A_e \qquad \textbf{(3)}$$

Further manipulating the equation by dividing both sides by the mass flow:

$$\frac{F}{\dot{m}_e} = V_e + \frac{(P_e - P_o)A_e}{\dot{m}_e} \quad \textbf{(4)}$$

The right hand side of the equation can represent a new velocity known as "equivalent velocity":

$$V_{eq} = V_e + \frac{(P_e - P_o)A_e}{\dot{m}_e} \quad \textbf{(5)}$$

We can further simplify the thrust equation to:

$$F = \dot{m}_e V_{eq} \quad \textbf{(6)}$$

Total Impulse for a rocket is defined as the average thrust of the motor times the total time of the thrust and is represented by:

$$I = F\Delta t \quad \textbf{(7)}$$

Since thrust is not constant over time we can integrate the total impulse with respect to time to yield:

$$I = \int_0^t F dt \quad \textbf{(8)}$$

Substituting equation 5 we get:

$$I = \int_0^t \dot{m}_e V_{eq} dt \quad \textbf{(9)}$$

Keeping in mind that $\dot{m}_e$ is the mass flow rate of the mass of the exhaust of the exiting from the rocket per time while assuming velocity stays constant; integrating the equation gives us:

$$I = mV_{eq} \quad \textbf{(10)}$$

Where m is the total mass of the propellant, the specific impulse can then be found by merely dividing the equation by the weight since the word specific simply means "divided by weight" given by:

$$I_{sp} = \frac{V_{eq}}{g_o} \quad \textbf{(11)}$$

Where g_o is the gravitational constant.

Substituting the velocity equivalent finally gives us the general specific impulse equation:

$$F_{thrust} = I_{sp}\dot{m}g_o \quad \textbf{(12)}$$

Note that specific impulse is measured in seconds.

There are many things to be considered in order to be successful and limit any chance of catastrophic failure. Along with using a solid propellant grain brings high pressure in the combustion chamber additionally with the combustion comes high temperatures. The team must account for the pressure in the tank at and elevated temperatures to prevent and breaches to the motor. A simple wall thickness calculation for a pressurized vessel can tell what wall thickness will be needed for the motor casing.

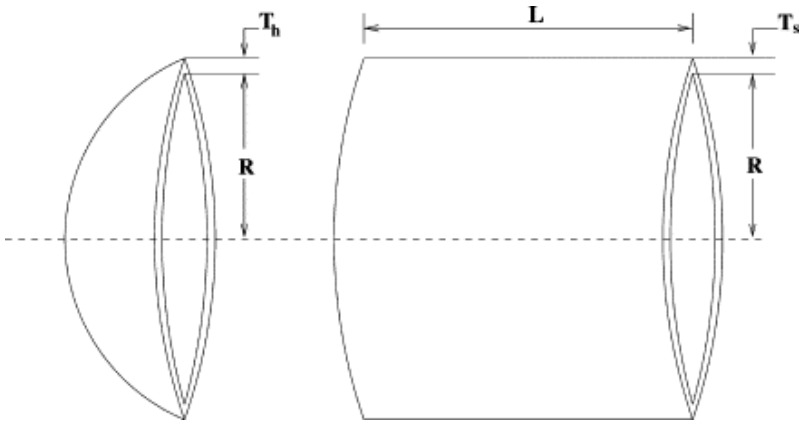

Figure 10: Cylindrical Vessel w/ Hemispherical Ends (Coello, 2002)

$$M = 2\rho R^2 (R + W) P \frac{r}{s} \quad \textbf{(13)}$$

Along with the elevated temperatures in the combustion chamber, heat is transferred to several components, mainly the bulkhead and injector assembly. It would be quite undesirable to elevate the temperature so high that the bulk transfers so much heat that it would elevate the oxidizer tank pressures to and undesirable rate. However, at the same time the heat transfer could be used as an advantage and heat the oxidizer as it passes though the injector to incase the enthalpy. The amount of heat transfer can be calculated using:

$$Q = v\rho C_p \Delta T \quad \textbf{(14)}$$

5.2. Nozzle Design

A nozzle's purpose is to expand the gas created within the rocket motor as efficiently as possible. One of the largest contributors to thrust loss within a rocket is due to the divergence half-angle of the nozzle. Due to this factor, consideration between three different nozzle types were both considered and compared. The three most common nozzle types used in rockets are the Bell-shaped nozzle (Figure 12), Annular nozzle, and Conical nozzle (Figure 13). The Bell-shape nozzle is amongst the most popular chosen design, and offers significant advantages over the other two nozzles. A Bell-shape nozzle contains a high angle expansion, between 20-50 degrees, behind the nozzle throat, while the exit divergence angle is usually less than 10 degrees. Although efficient, it is extremely difficult and costly to manufacture. An annular nozzle is theoretically considered to be the best option in rocket design. The nozzle's greatest attribute is its altitude-compensation, but this particular nozzle is extremely difficult to manufacture, and its complicated design creates great challenges for implementation. The team chose to go with the conical nozzle design due to its simplicity

and ease of construction. This particular nozzle gets its name from the constant angle created by the diverging walls. The nozzle's small angle produces a great thrust by maximizing the axial component of exit velocity, thus producing a high specific impulse. To ensure minimal thrust loss, it has been found that a divergence half-angle of 15 degrees leads to about a 1.7% decrease in thrust. A second contributing factor for loss in thrust, are throat type and size. The teams design calls for a straight drilled throat. The particular conical design chosen attributes an additional 3.3% loss of thrust. Although a total of 5% loss may be reduced to nearly zero with a well-designed Bell-shaped nozzle, the cost and difficulty in manufacturing it would not justify the minor increase in performance. Additional performance loss within the nozzle can total up to an additional 1%. This final loss can be attributed to the any friction loss within the nozzle. To find the throat size necessary for the conical nozzle designed, Equation (15) was used. (Kirk, Florida Institute of Technology) (Rogers)

$$A_t = \frac{F}{C_F P_C} \quad \textbf{(15)}$$

Where,

A_t = *Thrust Area*

F = *Thrust*

C_f = *Coefficient of Thrust*

P_c = *Chamber Pressure*

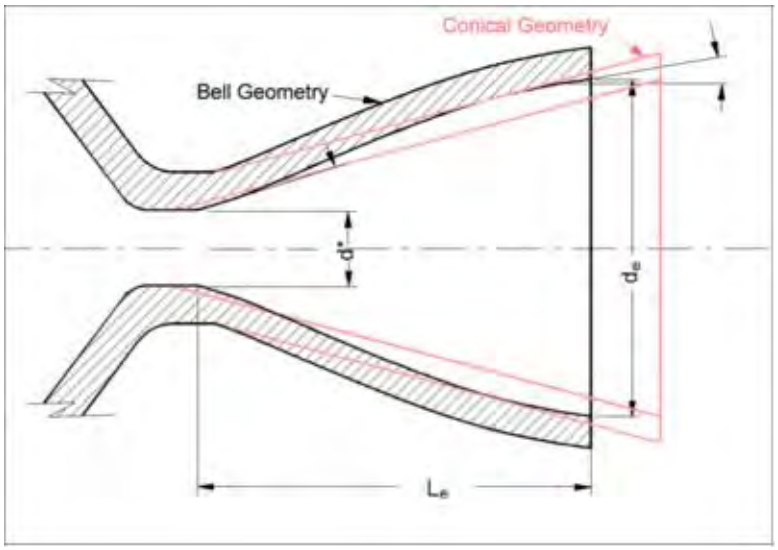

Figure 11: Bell-Shape and Conical Comparisson

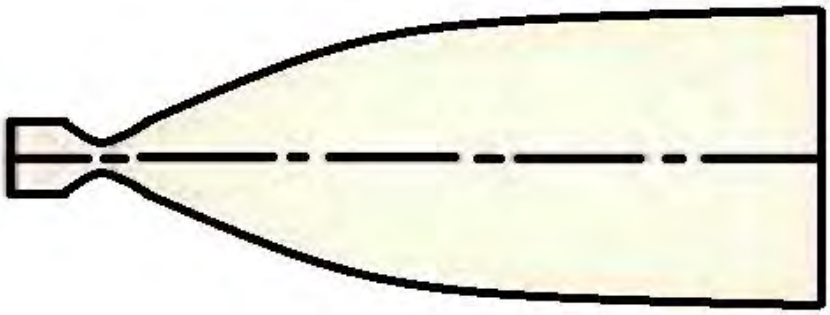

Figure 12: Bell-Shaped Nozzle

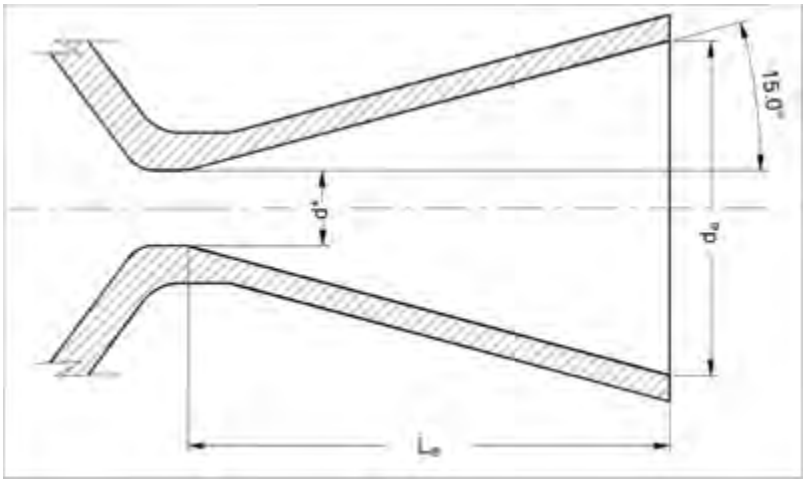

Figure 13: Conical Nozzle

5.3. Major Components

- Outer Casing
    - 6061-T651 Aluminum Tubing
    - Stainless 17-4PH Cone Tip
- Rocket Propellant
    - Solid Motor
        - HTPB Rubber Binder
        - Magnalium (Aluminum alloy with Magnesium and small amounts of copper, nickel and tin)
        - Ammonium Perchlorate (NH_4ClO_4)
        - Iron Oxide (FeO)
        - Black Carbon
    - Hybrid Motor
        - HTPB Rubber Binder
        - Magnalium (Aluminum alloy with Magnesium and small amounts of copper, nickel and tin)
        - Black Carbon
    - Carbon Layer
        - HTPB Rubber Binder
        - Black Carbon
- Oxidizer Tank
    - 6061-T651 Aluminum tank wrapped with Carbon Fiber
- Injector Nozzle

  - 6061-T651 Aluminum
  - Copper
- Telemetry
  - Altimeter
  - GPS
  - Go Pro
- Nozzle
  - Graphite nozzle
  - Phenolic
  - Aluminum Retaining Ring
- Fin Assembly
  - Aluminum Fins
  - Aluminum Can
  - Carbon Fiber Insert

5.4. Structural Design

The structure of the HySol rocket is composed of a hollow aluminum tube that will be filled with the rubber binder and it's ingredients to make up the two fuel grains; the hybrid and solid motor. The oxidizer tank will be joined to the casted motor casing though the aluminum bulkhead that will also be used as the injector. The cone will contain all telemetry and be located forward of the oxidizer tank. The Aft of the motor will be composed by the nozzle and throat assembly, which is retained by an aluminum-retaining ring. Attached to the outside on the Aft of the motor casing will be the Fin Assembly.

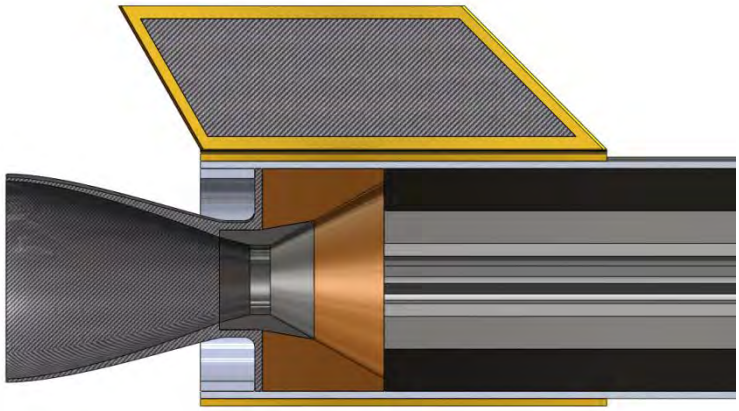

Figure 14: Aft of Motor

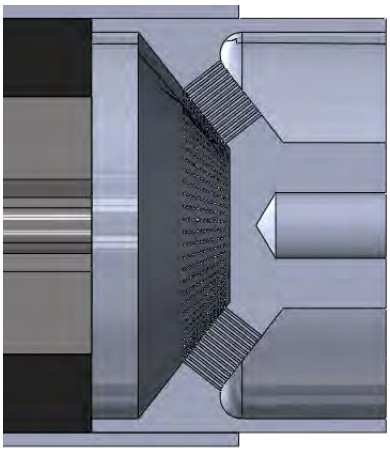

Figure 15: Injector Assembly

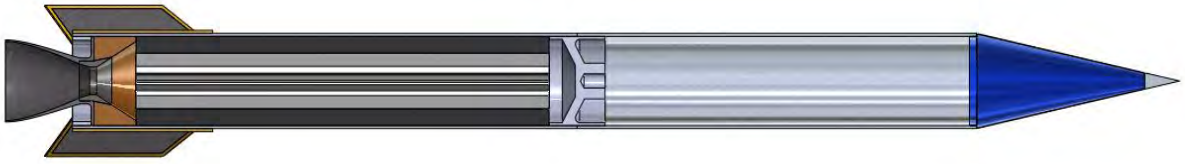

Figure 16: HySol Rocket Cross-Section

Figure 17: HySol Rocket

5.5. Cost Analysis

Table 3: Cost Analysis

Cost Analysis				
Items	**Unit price**	**unit**	**# of units**	**Total Cost**
Aluminum Tube Extrusions	$365.50	ft.	21	$7,675.50
Aluminum Cone	$400.00	piece	1	$400.00
Aluminum Sheet (18"x18"x1/4")	$86.57	sheet	2	$173.14
HTPB	$8.33	lbs	500	$4,166.67
Magnalium	$135.00	10 lbs	10	$1,350.00
Phenolic (12"X12"X1")	$89.13	piece	6	$534.78
Graphite (3" Diameter X 12")	$201.46	piece	1	$201.46
GPS	$100.00	piece	1	$100.00
Altimeter	$100.00	piece	1	$100.00
Resin	$75.00	quart	2	$150.00
Carbon	$40.00	yard	3	$120.00
Total				$14,971.55

6. Prototype Construction

6.1. Prototype System Description

The initial prototype for the rocket will be a scaled down rocket, which will consist of different parts joined together to form the entire system. The first two main components of the system are the internal two stage motors. The first stage is the solid motor and the second is the hybrid motor these two in conjunction will provide the entire driving force of the rocket. The top half of the rocket is an aluminum-extruded tube, which incases the rocket's oxidizing agent. Attached to the top of the rocket is the nose cone manufactured from a sheet of Aluminum rolled and then seam welded, the tip of the nose cone is made of stainless steel 17-7PH to help absorb the heat from the exorbitant speed the rocket will travel. The nose provides aerodynamic efficiency by allowing the rocket a smooth flight. The bottom half of the rocket is a second aluminum extruded tube. This is where the propellant is contained needed to provide the rocket with the greatest lifting force. Contained within the cylinder are the two stage propellant grains. The inner stage is the solid propellant casted onto the outer grain. The solid propellant is a carefully mixed composition of HTPB Rubber Binder, Magnalium, Iron Oxide, Black Carbon, oxidizing agent Ammonium Perchlorate and the catalyst to cure the mixture, Papi94. The solid grain is carefully molded with a star shaped hollow center known as a fin-o-cyl (fins on cylinder) providing the combustion chamber. The second stage which also uses the HTPB rubber binder, Magnalium and black carbon is casted first onto the aluminum tube casing this stages purpose will be to provide extra thrust to facilitate the a higher desired altitude.

6.2. Prototype Cost Analysis

Table 4: Prototype Cost Analysis

Prototyping Cost Analysis				
Items	**Unit price**	**Unit**	**# of units**	**Total Cost**
Aluminum Tube Extrusions	$46.73	ft.	12	$560.74
Aluminum Cone	$200.00	piece	1	$200.00
Aluminum Sheet (18"x18"x1/4")	$86.57	sheet	2	$173.14
HTPB	$8.33	lbs	100	$833.33
Magnalium	$135.00	10 lbs	2	$270.00
Phenolic (12"X12"X1")	$89.13	piece	2	$178.26
Graphite (2" Diameter X 12")	$119.00	piece	1	$119.00
GPS	$100.00	piece	1	$100.00
Altimeter	$100.00	piece	1	$100.00
Resin	$75.00	quart	2	$150.00
Carbon	$40.00	yard	3	$120.00
Total				$2,804.47

7. Oxidizer Injector Development Process

Concept 4 was the selected design to continue in the development process. The design calls for an array of seven small injectors that are plugged up with propellant and another material that prevents the chamber pressure from allowing the gases into the oxidizer tank. In order to obtain the necessary data to develop the final product a series of tests were performed. These were done with scaled down prototypes for cost saving reasons, environment control and safety precautions. The data gathered in these experiments assisted in the concept verification process.

7.1. Safety Considerations

Disclaimer: The HySol team (including the members and advisors shown on the cover of the report) does not disseminate nor certify the activities performed for the completion of this report as safe for the general public. Team HySol is not responsible for the actions, behavior or participation of the reader in the use and pursuit of the content existing on this thesis. He or she is solely responsible for practicing safety principles in order to keep the public safe.

The following safety summary reviews important points of attention that must be taken into account throughout any type of rocket motor construction. These do not encompass all the safety precautions that must be taken for the research and development of a motor. Please take into consideration at least the following safety precautions:

- **General Safety:** All the actions performed should have safety as the main objective. It is important to never become satisfied or over confident, and to always be prepare for an accident. It is important to be aware that propellants can ignite at any time, and one must be prepared to act accordingly.

- **Work environment:** The work location for the making of propellant should be well defined with no intrusion from equipment and/or materials not specific to the operation. The usage and measurement of raw chemicals should be done separately from the mixing process to avoid interaction. The chemical materials should be stored and locked in proper plastic containers when not in use. If possible, store the oxidizer and fuel in separate locations.
- **Neatness:** It is important to keep the area where propellant is being prepared and motors being fabricated, prepped, mixed and processed, clean and neat at all times. Special care needs to be taken with oxidizers, powdered metals, and other ignition sources to diminish the danger of inadvertent ignition. "Dusting" of fine materials should be avoided. Do not allow more than one container of chemical to be open at any given time.
- **Training:** Amateurs in their initial phases should always be under the supervision of an experience person. During this time one should only prepare mixtures that have been well characterized by others already.
- **Quantities:** amateurs should work with small amounts of materials. Uncharacterized experimental mixtures should not exceed 10 grams. Do not mix more propellant than the necessary for the project being manufacture.
- **Chemicals:** When handling chemicals one must become familiar with the Material Safety Data Sheet (MSDS) for each chemical used. Chemical incompatibilities must be known in order to avoid them (for example: aluminum and nitrates, and ammonium mixtures with chlorate mixtures).
- **Safety equipment:** Eye protection, respirator, and flame resistant clothing must be worn at all times. Always have water and foam type fire extinguisher, and a first aid kit handy.

- **Testing:** A new motor design should be static tested at least three times before committing the motor to fly. One should always be at least 75 feet from any motor being tested.
- **Motors:** Proper materials should always be used to manufacture rocket motors. The motors should be designed to fail longitudinal, a radial failure could be catastrophic. These motors should be tested vertically until the propellant has been correctly characterized. The motor should be designed to endure a minimum of 1.5 times the maximum expected stress.
- **Waste:** Scrap material and flammable waste should be disposed on a regular basis to avoid accumulation.

7.2. Procedures for Mixing Solid Propellant

Once the five prototypes were manufactured the next step was to create the solid propellant mixture. The following guidelines describe the propellant mixing process step by step.

1. Obtain the desired ratio for each material to be used in the mixture. For improved performance the mixture of Ammonium Perchlorate (AP) and metallic fuel (solids loading) should be stoichiometric close to 90%. However, such ratios are mostly used in professional rocketry. The following table illustrates an example of the material ratio used to create a propellant system. In this case 75% belongs to the oxidizer and metallic fuel while the remaining 25% belongs to the binding, plasticizing and curing agents.

Table 5: Rocket Fuel Composition

Material	Percentage
HTPB (Binder)	18%
DOA (Plasticizer)	5%
PAPI 901 (Curative)	2%
AP 400µ (Oxidizer)	36%
AP 90µ (Oxidizer)	36%
Metal (Zn, Al, etc.)	3%

2. Measure the desired volume of the motor to be filled with solid propellant.
3. After obtaining the desired volume to be filled and the percentage for each material, calculate the necessary weight fraction for each material (knowing that the desired density of the mixture is approximately 28 g/in^3).
4. Weigh each material on a separate plastic container.
5. Start mixing the materials in the same order described below. NOTE: Failure to follow the mixing process exactly as described will ruin the mixture if it goes dry.
    - Add the plasticizing agents, Dioctyl adipate (DOA), to the binder agent, Hydroxyl terminated polybutadiene (HTPB). This decreases the overall density of the mixture, allowing a higher solids loading while keeping the propellants pourable.
    - Stir the mixture until a homogeneous solution is obtained. This step will create undesirable air bubbles in the mixture.
    - To remove the air bubbles, place the mixture in a vacuum chamber. The necessary time to remove all the air bubbles will depend on the amount of mixture prepared.
    - Add the Ammonium Perchlorate (AP) 400µ grains to the mixture (coarse particles first). NOTE: It is crucial that the AP 400µ grains are added before the AP 90µ grains.

- Stir the mixture vigorously. At this point the density of the mixture starts increasing significantly.
- Add the AP 90μ grains and stir vigorously. Adding these grains will increase the density of the mixture substantially, therefore it is recommended to add them and stir the mixture in several steps.
- Add the metallic fuel to the mixture and stir vigorously. NOTE: This step should be performed carefully to avoid creating dust; which can create a safety hazard (propellant ignition) by static discharge.
- Add the curing agent, PAPI 901, to the mixture and stir vigorously. After adding the curing agent, it takes approximately 30 minutes before the propellant starts to set. At this point air bubbles have been created again in the mixture.
- Place the propellant mixture in the vacuum chamber to remove all the air bubbles. The necessary time to remove all the bubbles varies depending on the amount of propellant. NOTE: It is very important to remove all the air bubbles from the mixture. The propellant regresses equally in all directions, a trapped air bubble would increase the surface area of the burning propellant. A larger surface area would increase the pressure inside the motor and possibly cause failure of the system. Figure 22 illustrates the results of air bubbles trapped in the mixture.

6. Use a rubber spatula to scrape the walls and bottom of the mixing container.
7. Finally, pour the propellant into the desired motor carefully not to trap any air bubbles in the process, and then allow the propellant to cure overnight.

Figure 18 through Figure 21 show the propellant mixture being poured and casted into the test specimens used for test 1. It was very important to keep the propellant pourable to be able to properly cast it into the specimens.

Figure 18: Casting Test Specimens

Figure 19: Korey watching over Pedro casting the test specimens

Figure 20: Pedro Casting Test Specimen

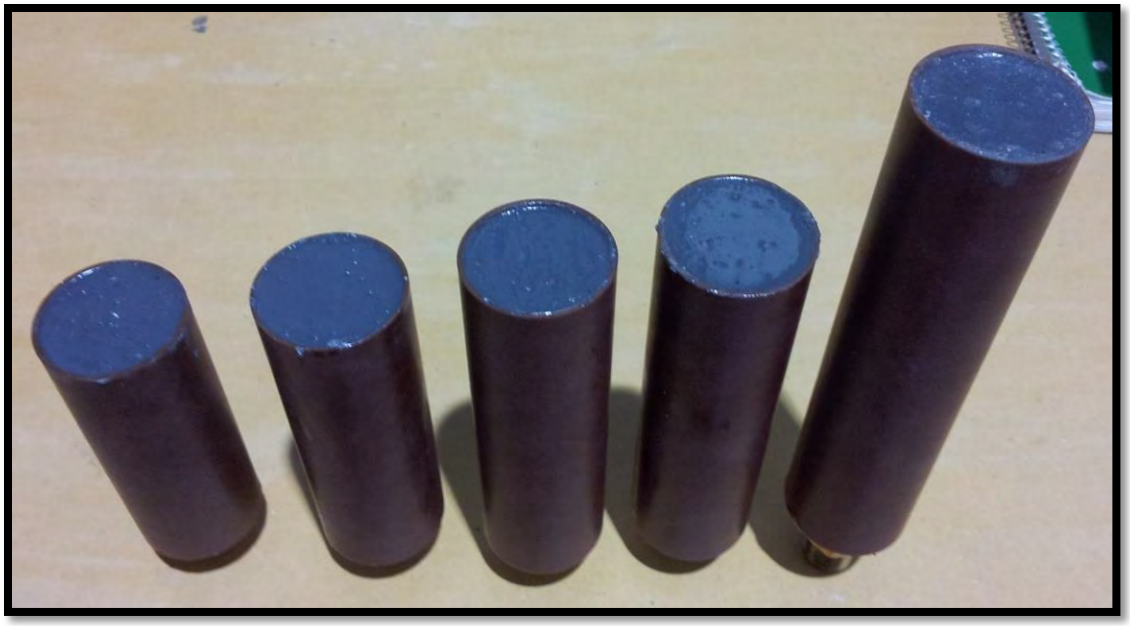

Figure 21: Final Casted and Cured Test Specimens

The prototypes were weighed before the solid propellant was casted into them. Once the propellant solidified the test specimens were weighed again to calculate the solid propellant weight. The density of the propellant was then found by using the weight of the propellant and the prototype volume. The calculated average density was approximately 24.34 g/in^3; however, the desired density was 28 g/in^3. It is presumed that there was too much HTPB in the mixture. In order to increase the density, more AP or metallic fuel can be added to the mixture.

Table 6: Test Specimen Fuel Density Data

Propellant Density			
Specimen No.	**Empty Weight [g]**	**Loaded Weight [g]**	**Density [g/in^3]**
1	73.7	197.6	24.08
2	75.6	217	24.42
3	80.1	244	24.46
4	NA	NA	NA
5	75.6	217	24.42
		Average	24.34

Figure 22: Effects of Trapped air bubble in solid propellant

7.3. Oxidizer Injector Test 1

Test 1 consisted of developing five different prototypes that provided regression rates and oxidizer commencement phase. The regression rate at atmospheric pressure and valve burst timing can then be used to estimate the regression rates at different chamber pressures.

7.3.1. Test Specimen design and fabrication

Figure 23 shows the CAD model of the first set of prototypes to be tested. The specimens consist of an aluminum valve attached to a phenolic casing. The solid propellant is to be encased in the phenolic cylinder, while the aluminum valve prevents the oxidizer from entering the chamber. The valve is made of a machined aluminum cylinder inserted into a compression fitting. The phenolic casing is made of a tube and a disc cut to a desired size.

The tip of the aluminum valve is thinner than the cylindrical walls; this permits the pressure in the tank to burst its tip and allow the flow of oxidizer. The burst occurs due to the lowered yield strength of the metal caused by elevated temperatures.

Figure 23: SolidWorks Test Specimen Model

An analysis was performed in SolidWorks Simulation before testing the valve, to replicate the testing conditions and predict the burst pattern. Figure 24 shows the results of the simulation, it can be seen that the valve will burst close to the tip.

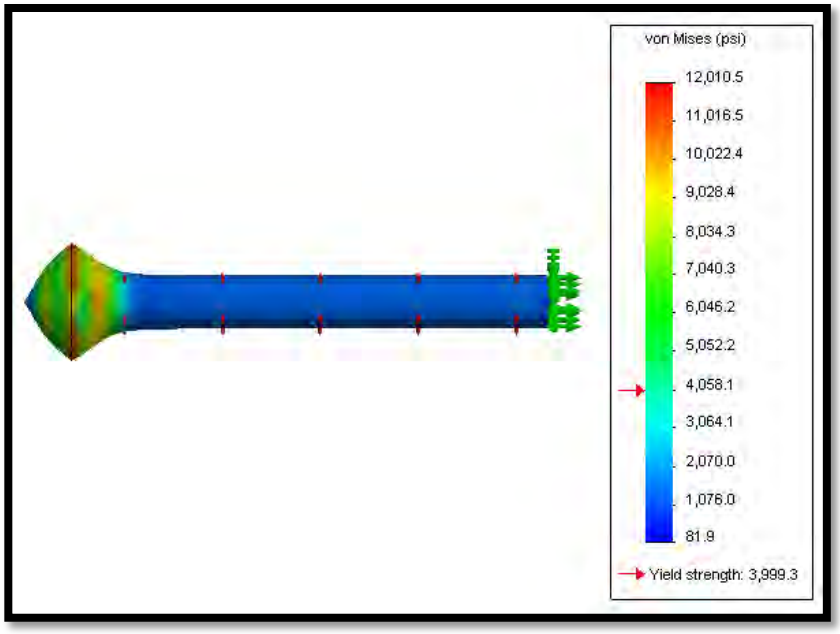

Figure 24: SolidWorks Valve Simulation

Figure 25 through Figure 28 show the fabrication process of the test specimens. The machining for all the parts was performed in the lathe.

Figure 25: Drilling I.D. on Phenolic Disk

Figure 26: Drilling I.D. on Phenolic Disk

Figure 27: Cutting off Phenolic Tube to Length

Figure 28: Pedro Drilling Phenolic Rod

Figure 29 shows an unassembled test specimen. The aluminum valve is shown on the left, and the phenolic casing is shown on the right.

Figure 29: Assembled Test Specimen Ready for Gluing

Once all the prototypes were assembled, they were pressured tested with argon to ensure that the valves could withstand the oxidizer tank pressure during the test.

Figure 30: Using Argon to Pressure test specimen

Table 7: Aluminum Valve Data

Aluminum Valve Dimension				
Tube length [in]	**O.D. [in]**	**I.D. [in]**	**Thickness [in]**	**Phenolic disk thickness [in]**
3.38	0.375	0.275	0.05	0.108

Table 8: Fully Assembled Specimen Dimensional Data

Test Specimens Dimensions					
Specimen No.	**Valve tip to open end length [in]**	**O.D. [in]**	**I.D. [in]**	**Casing length [in]**	**Volume [in^3]**
1	0.337	1.5	1.375	3.825	5.146
2	0.771	1.5	1.375	4.259	5.790
3	1.384	1.5	1.375	4.872	6.701
4	0	1.5	1.375	3.488	4.646
5	0.771	1.5	1.375	4.259	5.790

7.3.2. Test 1 Procedures and Results

With the test specimens prepared, the test development was initiated. First, the overall testing system was setup. It included a small-pressurized oxidizer tank that also held each individual test specimen. The small tank was filled with CO_2 or N_2O for their respective tests. Several safety precautions were implemented, a pneumatic valve was installed on the tank and this allowed it to be open and closed remotely. Also, CO_2 was used instead of N_2O for the first three tests. It was anticipated that carbon dioxide would extinguish the flame once the aluminum valve burst. Specimen No. 4 was the first to be attached to the pressurized tank for testing. Since the tip of the valve was flushed with the open-end of the propellant and phenolic casing, it demonstrated the regression rate of the propellant after having reached the valve system. The motor was ignited and allowed to burn until the pressure of the tank broke through the valve and allowed the CO_2 to flow freely. As expected, the increase in temperature lowered the yield strength of the aluminum, allowing the pressure to break through.

Once the control test was completed, the time taken for the CO_2 to flow was recorded. The time and length of propellant burnt to the point of released CO_2 was assumed to be consistent for each sample; which allowed for future regression rate predictions. Specimen No. 1 was also tested with CO_2. The process, in which the motor was ignited until flow of carbon dioxide, was repeated for a sample that had 0.337 inches of solid propellant on top of the valve tip. As expected, the burning time for the valve to burst took longer than the control test.

With the data from these two first tests the regression rates for the propellant before reaching the valve tip were estimated. To calculate it, the time taken for the valve to burst on the control test was subtracted from the burning time of specimen No. 1. Then the time was divided by the extra

length that the specimen had over the control specimen. With an estimated regression rate of approximately 0.05 in/s, the burn time for the next three test specimens was predicted.

Specimen No. 2 was also tested with CO_2, and it was predicted that it would burn for approximately 41.6 seconds. After the test was performed, the actual propellant burning time was recorded at 44 seconds.

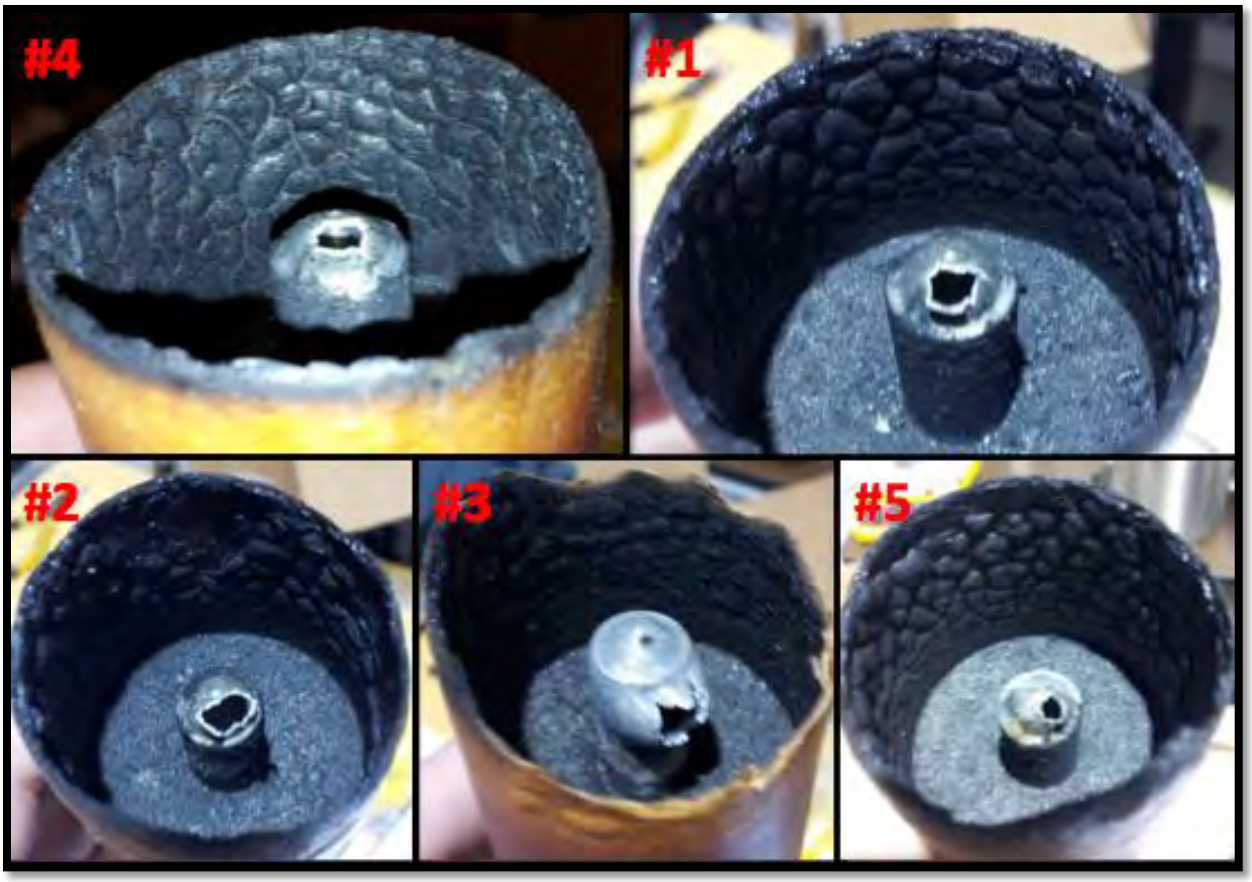

Figure 31: Test 1 specimens

After performing three successful tests on the samples, it was decided to replace the CO_2 with N_2O for the last two specimens. Test specimen No. 3 resulted in a longer burning time than expected due to a malfunction in the valve system. The valve malfunction was not determined, but it could be attributed to a manufacturing error or a heat transfer problem. For that reason it was not taken into account to calculate the average regression rate of the grain. Sample No. 5

was similar to sample No. 2, but this time nitrous oxide was used for the experiment. The estimated and actual burn time was 41.6 and 43 seconds respectively. The result of the two specimens showed a similar burn time.

Table 9: Test 1 Data

Test 1				
Specimen No.	**Estimated Time [s]**	**Actual Time [s]**	**Burn Length [in]**	**Regression Rate [in/s]**
1	32.24	31	1.038	0.056
2	41.57	44	1.565	0.041
3	54.75	65	2.178	NA
4	25	25	0.842	NA
5	41.57	43	1.538	0.0428
			Average	0.047

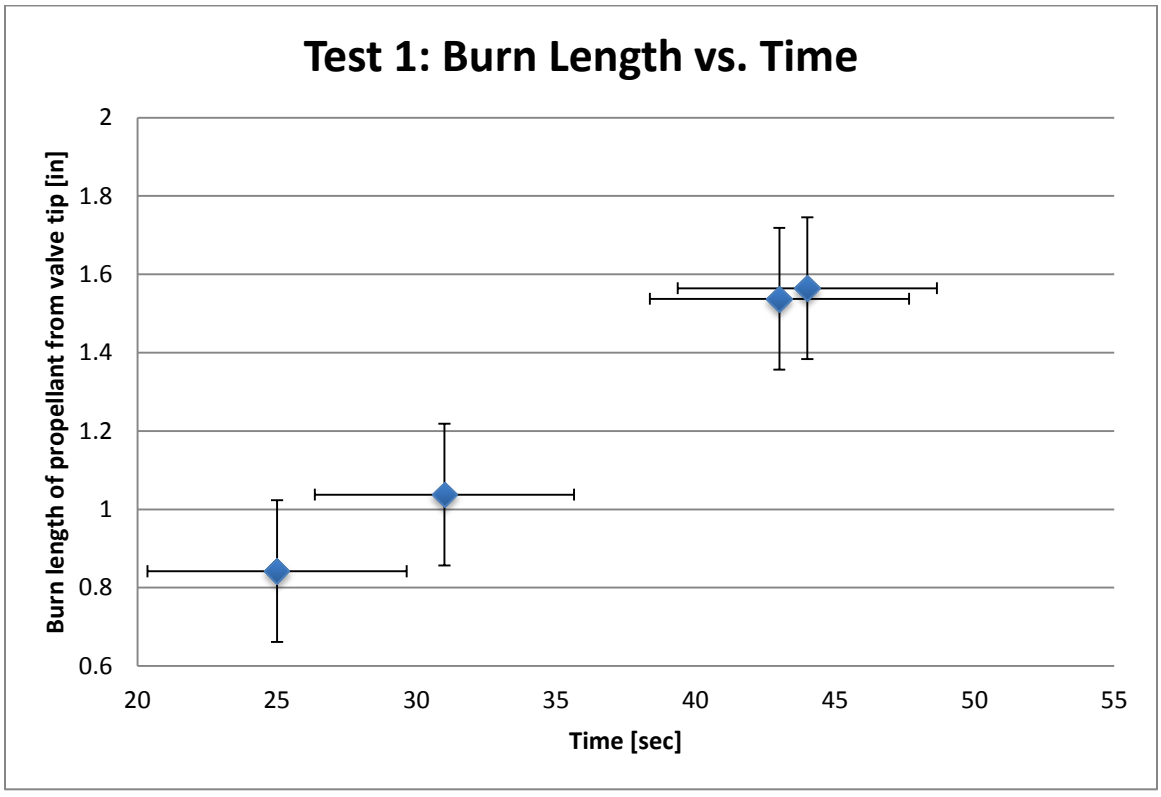

Figure 32: Test 1 Burn Length vs. Time

After gathering and analyzing the data for all the test specimens, the team became concerned with some of the results observed on the tested design. All of the specimens showed inconsistent rupture size on their respective valves. It is essential to have the same oxidizer flow rate for every valve system. Having different rupture sizes on the valves prevents the team from predicting the behavior of the system prior to propellant ignition. Another concern was that the nitrous oxide consistently extinguished the flame in the experiment. Figure 33 shows the burning solid grain on the right and the moment when the N_2O is released on the left. This behavior was not predicted beforehand, on the contrary, it was expected to obtain a hotter flame when the N_2O was combined with the solid grain.

Also, the amount of propellant before the tip of the valve can be adjusted as desired. It can be observed in Figure 32 that a longer distance will take more time to burn before reaching the tip of the valve. Finally, it was noted that the valve system size could be reduced, because there was a significant amount of unburned solid propellant left after the valve opened.

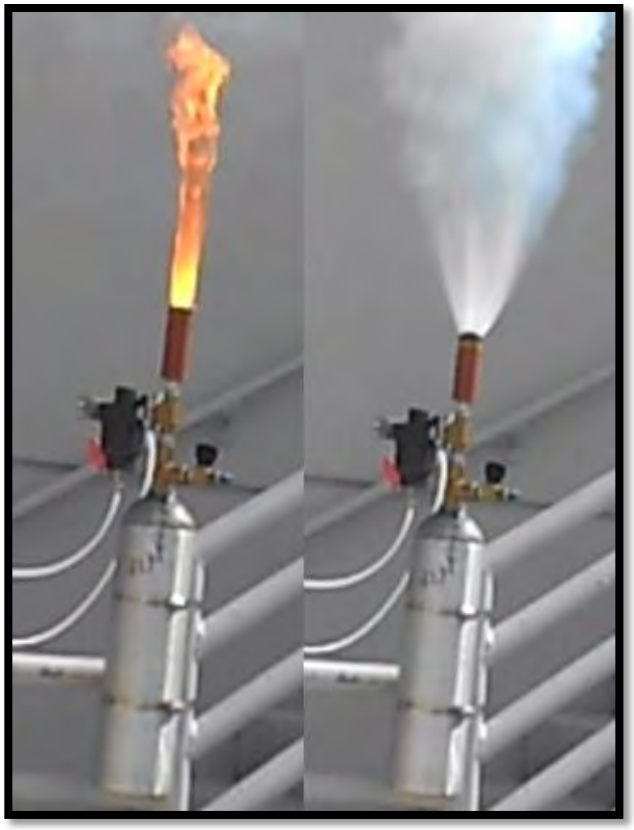

Figure 33: Using N_2O for Test 1

7.4. Oxidizer Injector Test 2

Test 1 confirmed that solid propellant could be used to activate the valve that commences the second stage hybrid motor. However, the inconsistency in the size of the burst orifice and long delay to trigger the start of the hybrid stage called for a new valve design.

7.4.1. Test Specimen Redesign

Oxidizer flow rate consistency was the main requirement needed to fulfill in the redesigned valve system. In order to achieve this parameter the generated orifice diameter on the valve had to be the same for every test. Figure 34 shows the CAD model of the test specimen used in test 2, which include the redesigned valve. The test specimens are similar to those used in test 1. The

solid propellant is enclosed in a phenolic cylinder and it acts as the trigger mechanism for the valve that allows transition to the second stage hybrid motor. A brass valve was capped with a low melting alloy to prevent the nitrous oxide from entering the chamber during the solid rocket stage. The composition of the bismuth alloy is shown in Table 10: Bismuth Alloy Composition this material expands about 3% of their volume when changing from liquid to solid. The low melting alloy melts soon after the solid propellant exposes it to the flame, allowing the oxidizer to enter the combustion chamber and start the hybrid phase.

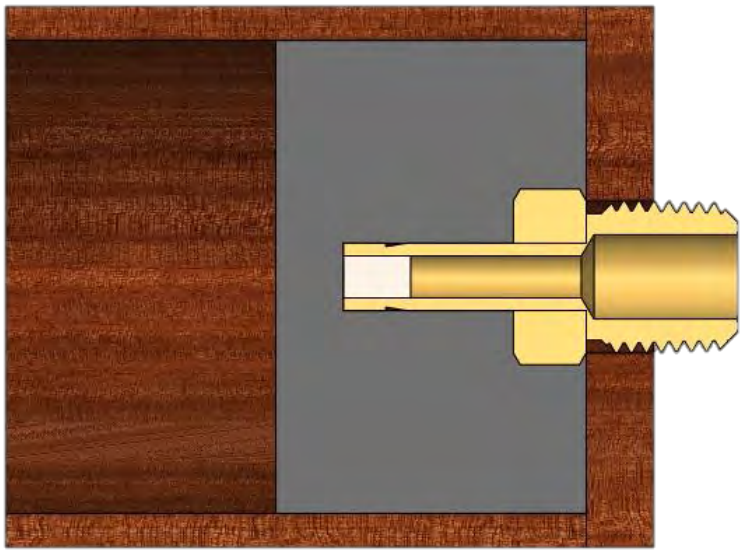

Figure 34: Specimen for Test 2

Table 10: Bismuth Alloy Composition

Melting Temperature [F]	Bismuth	Cadmium	Lead	Tin
158	50%	10%	26.7%	13.3%

The plug needed to withstand 750 psi from the nitrous oxide plus 43 psi from the g-force created during takeoff. The pressure related to the g-force varies according to the length of the tank and the diameter of the plug. It was not known how much pressure the low melting alloy would hold when casted inside the brass tube fitting. Therefore, the first task performed before assembling

the test specimens was to test the new valve setup for maximum allowable pressure. The low melting alloy was casted and then machined to a thickness of 0.5, 0.25 and 0.125 inch respectively. A pressure regulator was used to regulate the pressure of the nitrogen used for the test. All the valves were able to hold 1,000 psi. It was then decided to go one step further and test a valve with a thickness of 0.0625 inch, which also held 1,000 psi. The reason these valves can hold so much pressure is because the low melting alloy is a material with negative thermal expansion properties. This type of material contracts upon heating, therefore the alloy expanded once casted and hardened inside the brass valve.

Table 10 shows the dimensions of the specimens manufactured for the test. There are six small diameter specimens and three big diameter specimens. Prototype "large 1" has a different configuration, a small phenolic tube was inserted into a larger one, and both were filled with propellant. Also, a hole with a 0.75 inch diameter, 2 inches deep was drilled on the center of specimen "large 3" to allow for some back pressure to build. The team was trying to observe if these configurations would allow the flame to stay lit once the N_2O was released.

Table 11: Test 2 specimen dimensions

Specimens Dimensions						
Specimen No.	**Propellant length after valve tip [in]**	**Metal length in valve [in]**	**O.D. [in]**	**I.D. [in]**	**Inside length [in]**	**Inside Volume [in^3]**
1	0.179	0.174	1.5	1.375	1.385	2.057
2	0.548	0.166	1.5	1.375	1.748	2.596
3	0.22	0.308	1.5	1.375	1.428	2.120
4	0.516	0.37	1.5	1.375	1.72	2.554
5	0.208	0.371	1.5	1.375	1.41	2.094
6	0.538	0.185	1.5	1.375	1.754	2.605
Large 1	0.775	0.263	1.5/2.25	1.375/2	1.97/1.31	4.726
Large 2	1.1	0.269	2.25	2	2.3	7.226
Large 3	2.35	0.27	2.25	2	3.61	11.341

The specimens for test 2 were weighed before the solid propellant was casted into them. Once the propellant solidified the test specimens were weighed again to calculate the solid propellant weight. The calculated average density was approximately 23.47 g/in^3, which is somehow different from the density obtained for the propellant mixed in test 1. Extra Ammonium Perchlorate was added to the propellant used in prototype 6 to make the flame hotter.

Table 12: Test 2 Average densities

Propellant Density			
Specimen No.	**Empty Weight [g]**	**Loaded Weight [g]**	**Density [g/in^3]**
1	57.8	104.8	22.85
2	60	120.2	23.19
3	58.6	107.4	23.01
4	61.4	121	23.34
5	60.8	108.4	22.73
6	59.8	118.4	22.50
Large 1	94.6	208.4	24.08
Large 2	100	278.6	24.72
Large 3	123.4	404.2	24.76
		Average	23.47

Figure 35 shows specimen “large 3” moments before ignition. An electric match acts as the ignition source, which lights the solid grain from the bottom of the hole.

Figure 35: Specimen "large 3"

7.4.2. Test 2 Procedures and Results

The overall system setup for test 2 was similar to the system setup used in test 1. The small pressurized oxidizer tank this time was attached to a different valve system. For this test, the tank was filled with nitrous oxide from the start. Specimen No. 1 was the first one to be tested. The specimen burned for approximately 9 seconds before being put out by the release of N_2O. Once the flames were off the team took a closer look at the test sample and the results were positive. The low melting alloy plug was completely gone, leaving a uniform hole in the valve. Figure 38 shows the samples after being tested. Specimen No. 3 and No. 5 were then tested; they burned for 14 and 12 seconds respectively. The results were similar to those obtained for specimen No. 1. Once again, the nitrous oxide put off the flames and a uniform hole was obtained when the plug melted. It was then decided to test specimen “large 2” since it had a bigger propellant surface area; this could help keeping the flame lit after the oxidizer was released. The sample burned for approximately 35 seconds before being turned off when the oxidizer was released.

Figure 37 shows the configuration of specimen “large 1”; which was modified in an attempt to keep the flame lit after releasing the oxidizer. The specimen is composed of two concentric phenolic tubes that are filled with propellant. The propellant on both tubes was ignited and the inside cylinder burned for 29 seconds before the oxidizer was released. The flame on the inside cylinder was extinguished, however, the outside cylinder stayed lit. The desired result of igniting the flowing oxidizer had once again failed. It was determined afterwards that the flame stayed lit because it was protected by the inside cylinder and it was burning bellow the tip of the oxidizer valve. One final attempt was performed to try to keep the flame on after releasing the oxidizing agent. A 0.75 inch diameter hole 2 inches deep was created in specimen “large 3”. This would create an even larger surface area along with some backpressure. The solid grain burned for approximately 18 seconds and it was once more extinguished when the oxidizer was released. At this point, it was apparent that the oxidizer would not light on with the current configuration. However, specimens 2, 4 and 6 were still tested to acquire an average propellant regression rate.

Table 13: Test 2 data

Test 2			
Specimen No.	**Burn Time [s]**	**Burn Length [in]**	**Regression Rate [in/s]**
1	9	0.319	0.0354
2	20	0.6675	0.0334
3	14	0.422	0.0301
4	24	0.71	0.0296
5	12	0.4155	0.0346
6	20	0.6785	0.0339
Large 1	29	NA	NA
Large 2	35	1.233	0.0352
Large 3	18	0.463	0.0257
		Average	**0.0323**

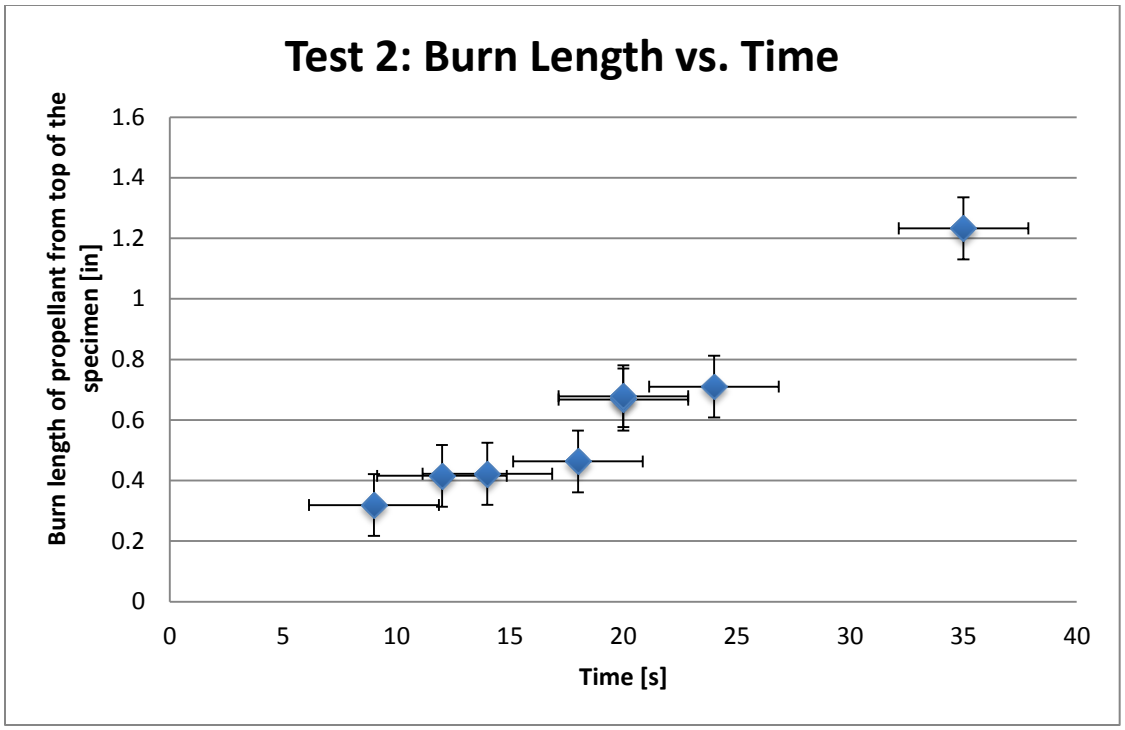

Figure 36: Test 2 Burn Length vs. Time

Figure 37: Test 2 Specimen "large 1"

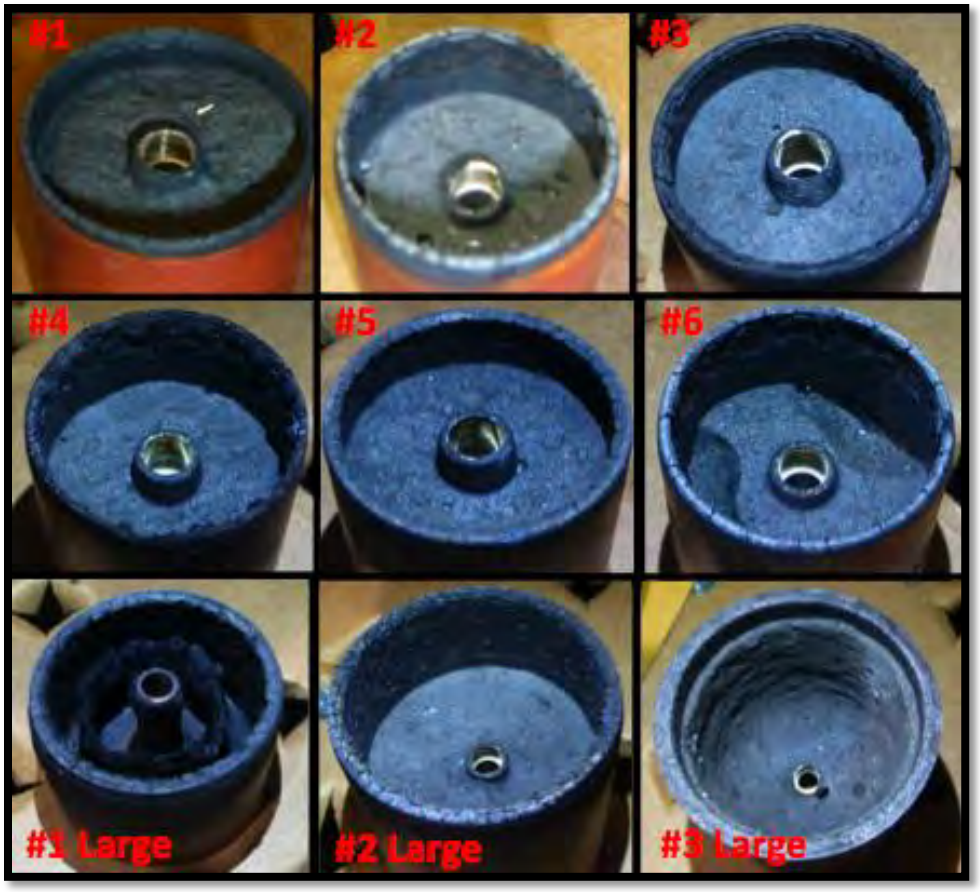

Figure 38: Specimens Test 2

The alloy plug melted almost instantly after being exposed to the flame; therefore, it was determined that the amount of solid propellant needed bellow the valve tip was very small. It was also decided to use 0.25-inch alloy plugs for future testing, since they are easier to manufacture. The results obtained in test 2 were successful even when the team was not able to ignite the oxidizing agent after being released. Using a solid grain to trigger the opening of the oxidizer valve, while maintaining a constant size orifice, was a giant leap in the development of the final product. With the redesigned valve system the same oxidizer flow rate could always be achieved.

7.5. Oxidizer Injector Test 3

Test 3 focused on the successful ignition of the hybrid phase, after the oxidizer flow was triggered by solid propellant. The same redesigned injector used for test 2 was used this time. The team learned that during the past two tests, when the oxidizer was released, there was no fuel to initiate the combustion process. One of the three essential elements of combustion had been overlooked. A simple cost effective approach to test the hybrid phase was to make a motor out of PVC tubing. It would provide the fuel necessary to initiate the hybrid motor and it would also serve as the casing. Since PVC has pressure limitations, the only calculation needed at this point was maximum chamber pressure. The schedule 40, 3 inch PVC tube used was rated at 250 psi; therefore the motor was designed to run at around 150 psi. Adjusting the nozzle throat area easily controlled the chamber pressure. Figure 39 shows the CAD modeling of the hybrid motor to be tested. The oxidizer injector can be seen completely covered with solid propellant. Also a PVC reduction coupling is used to create a converging nozzle.

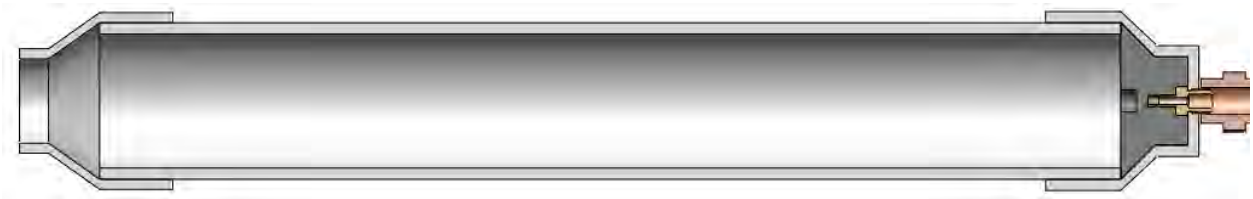

Figure 39: Test 3 CAD Model

An average regression rate of approximately 0.03 in/sec had been obtained experimentally in test 2; therefore a 0.5 inch hole was drilled to position the oxidizer injector tip 0.315 inches below the propellant surface. It was then estimated that oxidizer flow would start approximately 11 seconds after ignition. This would warm up the combustion chamber and allow better initial combustion of the hybrid phase.

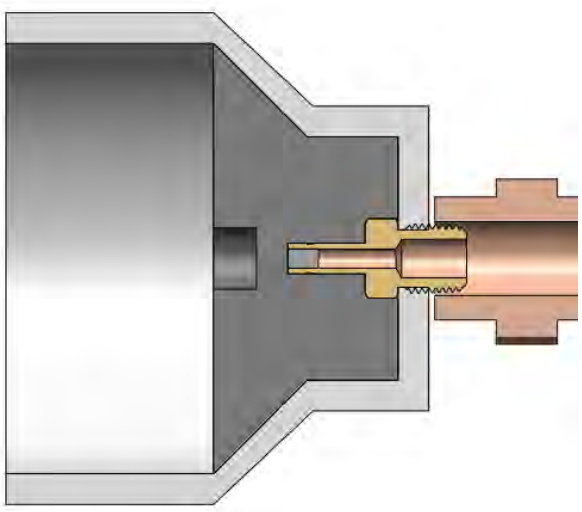

Figure 40: Test 3 Injector CAD Model

The test successfully proved that solid propellant could be used to initiate oxidizer flow and start a hybrid motor. Figure 41 shows the hybrid motor at three different instants after being commenced. The hybrid stage started approximately 12 seconds after the ignition of the solid propellant. The team had estimated a burn time of 11 seconds before hybrid stage ignition, which is close to the actual burn time. The difference between the actual and predicted time could be due to minor disparities in the solid propellant mixture. The hybrid motor burned for approximately 7 seconds.

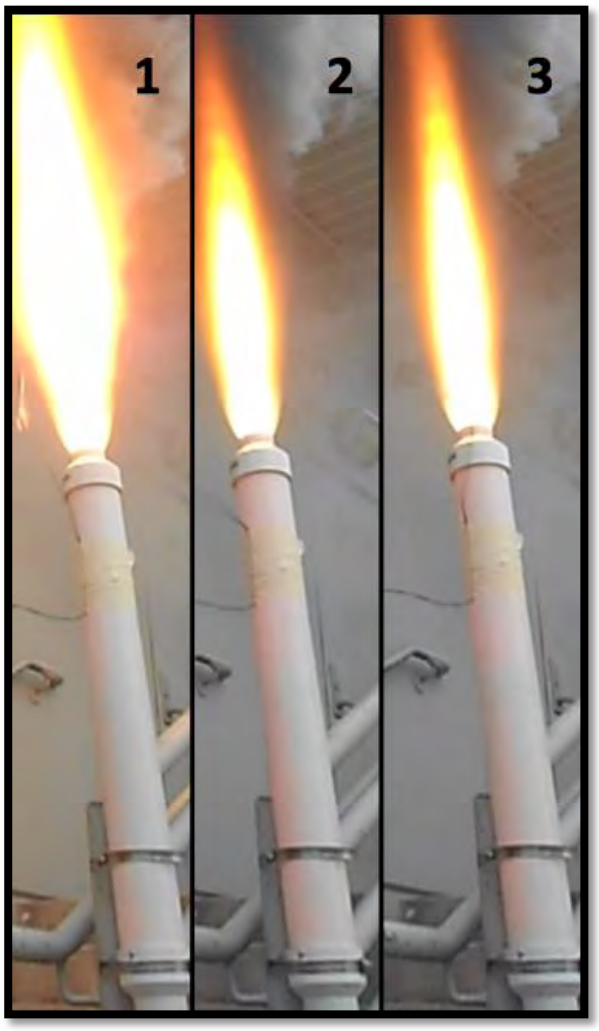

Figure 41: Test 3 Hybrid Motor

The team decided to perform a second test, a clear PVC tubing acted as the fuel and casing. Figure 42 shows full vision of the complete process, from the ignition and burn of the solid grain to the flow of oxidizer on the hybrid stage. It was calculated that the solid grain would burn for about 9.79 seconds before initiating the hybrid phase. The actual time was 10 seconds. The regression rate had been adjusted to 0.02625 in/sec, which was the actual regression rate of the previous test. The burning time of the hybrid stage was also 7 seconds for this test. Figure 43 shows the clear PVC motor dissected view, it could be seen that very little fuel was consumed in the hybrid phase.

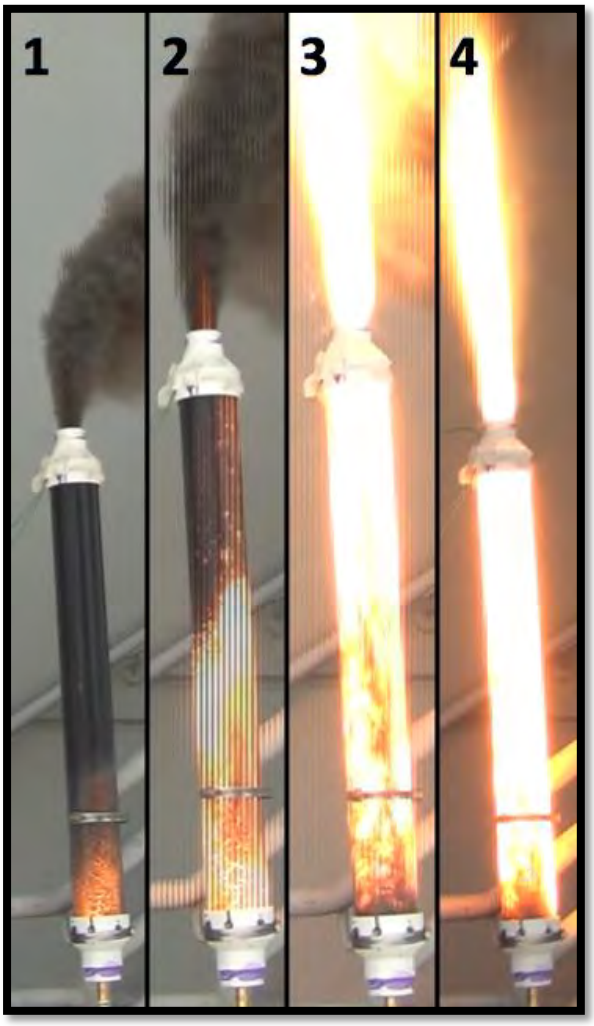

Figure 42: Test 3 Clear PVC Hybrid Motor

Figure 43: Clear PVC Hybrid Motor Dissection

8. Prototype Testing Plan

Prior to constructing a small-scale rocket to fly, the team developed a series of scaled static tests, in order to verify the transition of solid to hybrid rocket. An initial test was performed on the hybrid motor only to obtain pressure and thrust data. After the test was performed successfully, the team decided to perform a solid and hybrid motor test. With the use of the facility and guidance of the corporate sponsors, the team acquired data to verify thrust transition and characterize the propellant used.

8.1. Test Stand Design and Fabrication

The team's initial step was to design a SolidWorks model of both the scaled test rocket and vertical test bench, to ensure both would be modeled to real life standards. Figure 44 below demonstrates the initial scaled rocket, which would be designed and tested. To the left of the image is the oxidizer tank which will be used during the scaled static test. The solid motor pictured to the right is designed to a 3" diameter. The entire test rocket will sit vertically into a static test stand.

Figure 44: SolidWorks Scaled Model

Once the design for the static test rocket is complete, the test bench can then be modeled. Knowing what materials were readily available to the team, an overall idea was designed in SolidWorks. The base of the test stand is a tripod design to maximize stability to every direction. The cylindrical base open on both ends, will house the oxidizer tank during each test. The bottom of the base is attached to a bulkhead, which will support the downward force produced from the

rocket. The bulkhead is attached to an S beam load cell which reads the amount of force produced by each rocket. In order to ensure snug fit of the oxidizer tank, and avoid lateral movement during testing, a thin circular disc made of phenolic is cut to fit between the gaps produced. Each leg of the base will also house a ¼" metal wire, which will also be used to hold the rocket from any extra lateral movement. Figure 45 demonstrates initial model for the static test stand.

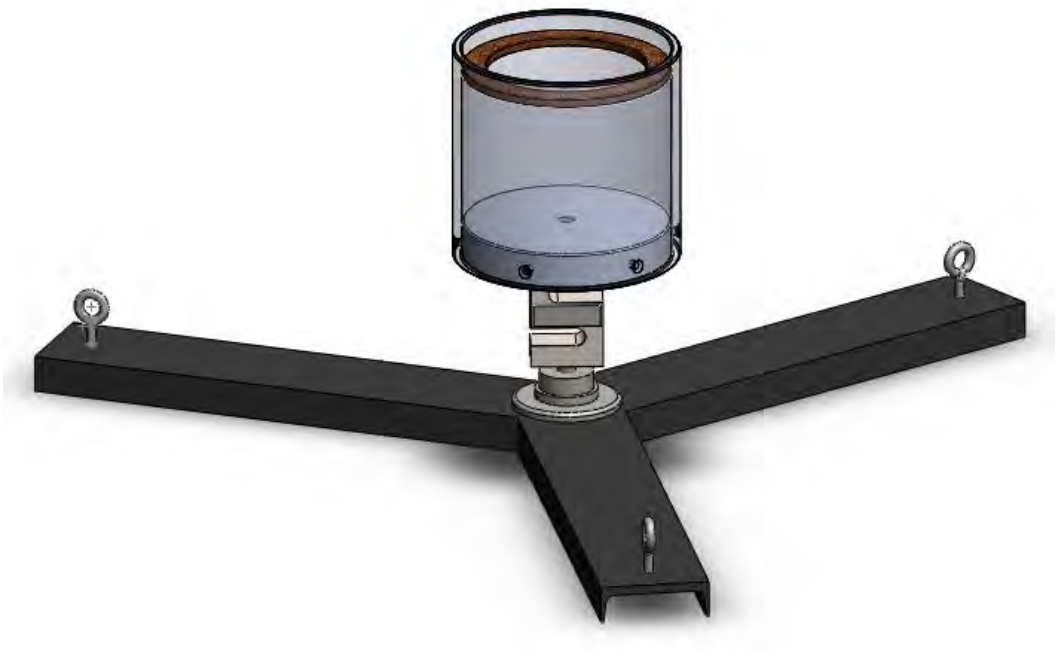

Figure 45: SolidWork Test Stand design

Figure 46 demonstrates how the overall test stand was designed, with the test rocket attached, as well as the wires clamped to ensure stability.

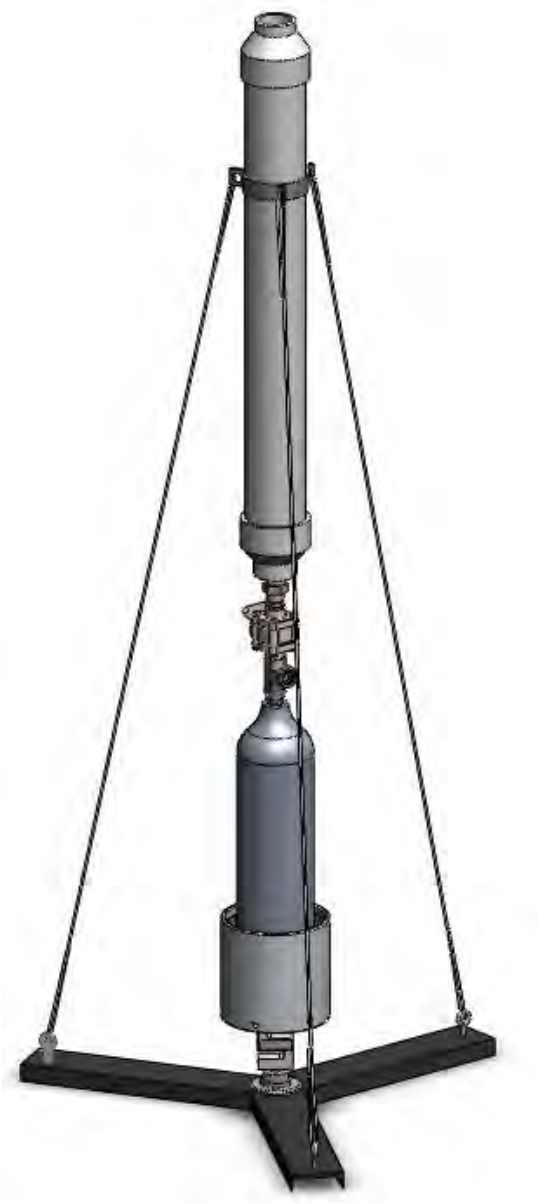

Figure 46: Test Stand with Test Rocket

Figure 47 demonstrates the test stand built by the team. The tripod base is manufactured of a single steel base. The housing cylindrical base was manufactured to hold a majority of the oxidizer tank, to ensure a more stability within the test. A pressure gauge was also mounted to the test rocket to allow compared pressure readings between the pressure transducer and itself.

Figure 47: Actual Test Stand with Rocket

To accompany the test stand, a control box, Figure 48, was constructed to house all necessary pneumatic valves, as well as an ignition switch. Originally not housed together, the two pneumatic air control valves were individually held. Each pneumatic valve is set to naturally close, which ensures quick closure during any unexpected event. The first valve controls the flow of the oxidizer tank, while the second controls a separate Carbon dioxide tank. The tank allows a quick release of a cold compressed gas into the system. The cold gas quickly extinguishes any

lingering flames which may have stayed lit during testing, thus preserving the motor for posttest observations. The final component contained within the control box is a momentary switch. The switch provides a quick connection and ignition to the low resistance electric match used to light the rocket.

Figure 48: Control Box

8.1.1. Data Acquisition

In order to effectively find the amount of force and pressure being produced by the rocket being tested, a data acquisition interface was formed. The hardware used to obtain the necessary data from the test stand was the Omega OMB-DAQ-3005. This particular system was readily available, and was paired with a free trial version of DasyLab 12.0. Connected to our DAQ system are two analog sensors that collected the necessary data. The sensors being used are an Omega LC101 load cell to measure force, and an Omega PX-602 pressure transducer to gauge pressure. Each individual sensor forwards signal data received to the DAQ system, which is then interpreted through the written DasyLab worksheet and converted into useful data. The signal

received into the DAQ system from the analog sensors is a voltage signal. Figure 49 shows the DasyLab worksheet, which was specifically written for the designed test bench.

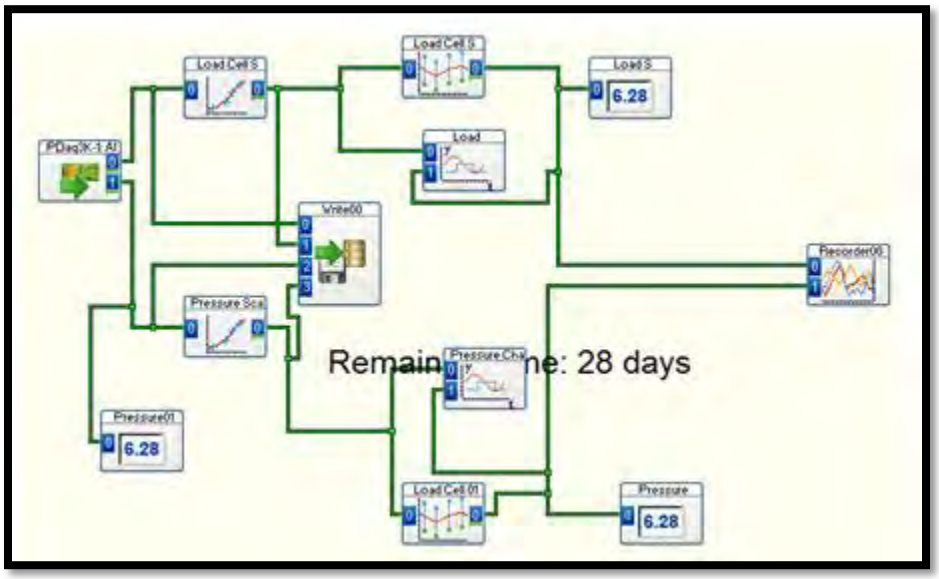

Figure 49: DasyLab Worksheet

Figure 50 focuses on the load cell sensor portion of the worksheet. The DAQ system receives a signal from the load cell, which is sent into a function module within the DasyLab worksheet. The worksheet interprets the initial signal data and converts it into needed functional data.

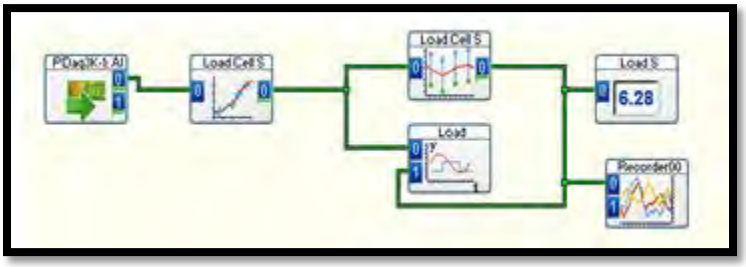

Figure 50: Load Cell Worksheet

Table 14: Load Cell Specification

Excitation Voltage	Output Voltage	Load Cell Range
10 V	3 mV/V	0-2000lbf

Knowing the range the load cell is capable of handling, as well as the output range, the first set of parameters can be calculated as follows:

$$\frac{2000lbf}{10 * .003} \quad \textbf{(16)}$$

This value scales the voltage signal received from the load cell and allows the desired form of pounds-force to be displayed. Once the DasyLab worksheet is set to display the force measured, calibration is needed to insure accurate data is obtained. An Arbor Press and a Mark 10 force gauge was placed in line with the load cell for initial calibration. Different forces were measured between both the load cell and Mark 10, which resulted in a needed overall calibration of 20lbf. Figure 51 demonstrates the pressure transducer portion of the DasyLab worksheet. Similar to the load cell, the pressure transducer outputs a voltage signal that is then interpreted by the worksheet. The pressure transducer's known pressure reading range and output range can be seen in Table 15: Pressure Transducer Specification.

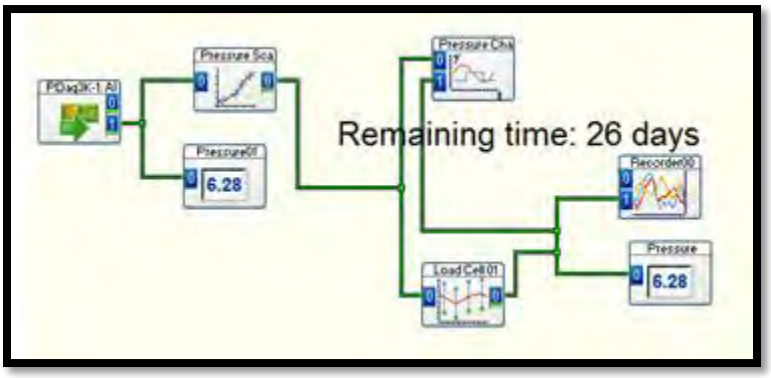

Figure 51: Pressure Transducer Worksheet

Table 15: Pressure Transducer Specification

Excitation Voltage	Output Voltage	Pressure Transducer Range
10 V	100 mV	0-1000 psi

Using this information, we can form parameters to convert the given signals into psi.

$$\frac{1000psi}{10V * .1mV} \quad \textbf{(17)}$$

Once the known parameters are ready to be read by the DasyLab worksheet, calibration must be done to ensure proper pressure is being read. By attaching a pressure regulator and a CO_2 tank alongside the pressure transducer, a list of different pressure readings can be compared and adjusted.

Once calibration is complete for the load cell and pressure transducer, the overall worksheet can be tested to ensure proper data is being received and interpreted properly. Initial tests ran from the worksheet showed sporadic data, which made no sense and was not to be expected. Most of this was attributed to two factors, a high number of data points and noise from the connected laptop. Noise as referred to here, is a random fluctuation in an electrical signal. The high number of data points allowed all the noise being received to be included in the resulting data. In order to help prevent unwanted data from the results, averaging modules were included in both force and pressure parameters. The amount of data points collected in the worksheet was lowered to 100 points a second. By doing so, the chance of collecting noise as part of the data set was minimized. The most important module in our worksheet writes all the data interpreted into a separate excel file. This allows the data to be read and graphed individually between tests.

8.2. Hybrid Motor Test

The team decided to perform a full test on the hybrid motor. The test consisted on analyzing the thrust and pressure profile of the hybrid stage. As in the two previous tests, solid propellant was used to trigger the pyrotechnic valve that initiates the hybrid motor. Several calculations were performed to anticipate the performance of the rocket during the test. The following equations drove the design process:

Oxidizer mass flow rate:

$$\dot{m} = C_d A_i \sqrt{2\rho_o \Delta P g} \quad \textbf{(18)}$$

Where C_d is the coefficient of discharge, A_i is the oxidizer injector cross-sectional area, ρ_o is the oxidizer (N_2O) density and ΔP is the pressure difference between the oxidizer tank and the combustion chamber. The weight of the oxidizer was measured before the test to confirm the estimate the mass flow rate after the test.

Oxidizer injector velocity:

$$V_i = C_d \sqrt{\frac{2\Delta P g}{\rho_o}} \quad \textbf{(19)}$$

Table 16: Hybrid Motor Anticipated Performance shows some of the values the team expected to obtain during the test. There are several values that are assumed, and they could cause erroneous approximations. For example the oxidizer to fuel ratio was approximated to be 4:1. These assumed values were obtained from previous experiences the team's industry advisors had.

Table 16: Hybrid Motor Anticipated Performance

Injector I.D. [in]	0.25	
Injector Area	0.0491	
C_d	0.6	
Density N2O [lbs/in^3]	0.0231	
Pressure Drop [psi]	80	
Gravity [in/s^2]	386.088	
Mass Flow [lbs/s]	1.11	
Injector Velocity [in/s]	980.16	
N2O (oxidizer) weight [lbs]	4.78	O/F ratio 4:1
Fuel weight [lbs]	1.19	
Specific Impulse [s]	200	120
Total Impulse [lbs-s]	1194.38	718

Assumed	Experimental Values
Calculated Value	

One more time, a schedule 80, 3 inch PVC tube was used as the motor fuel and casing. The pipe was rated at 500 psi, and the expected pressure chamber was approximately 150 psi. In Figure 52 and Figure 53 the motor bulkhead can be observed. The center brass piece is the oxidizer injector, while the two aluminum tubes on the side are for pressure gaging. HTPB was also added to the bottom of the bulkhead to isolate the heat coming from the burning solid propellant. A PVC reducer coupling was used as the motor nozzle, making the throat diameter 1.625 inches. This helped maintained the chamber pressure during the hybrid stage. The estimated total impulse of the motor is 1194 lbs-s. This means that the motor could output 1194 lbs of thrust for 1 second, or 109 lbs of thrust for about 11 seconds.

Figure 52: Motor Bulkhead

Figure 53: Motor Bulkhead with HTPB

Figure 54 shows two different views of the hybrid motor while being tested. The test was conducted without any motor complications. The solid grain triggered the pyrotechnic oxidizer

injector, and the hybrid motor burned for about 14 seconds. Unfortunately, the pressure transducer and load cell were not able to obtain data. There was an unexpected source of noise that did not allow the data to be readable. The source of noise was detected and avoided in future tests. A pressure gauge had also been installed in the test stand to read chamber pressure. Since the experiment was recorded the team was able to obtain pressure readings from this gage.

Figure 54: Hybrid Motor Test

The video obtained captured 30 frames per seconds; therefore there are 30 pressure readings per seconds. Figure 55 shows the pressure and thrust profile of the hybrid motor. The moment at which the oxidizer injector is open by the solid grain can clearly be seen in the graph. The chamber pressure went from 0 to 130 psi in less than 0.02 seconds. The pressure slowly decreased for 2.27 seconds. After that point the PVC nozzle started eroding, substantially

increasing its diameter and therefore reducing the chamber pressure. The thrust output was calculated using Equation (15), the throat diameter and chamber pressure were known, however, the thrust coefficient was assumed. Thrust is proportional to the chamber pressure; therefore their profiles are similar. The total Impulse estimated from the graph is approximately 718 lbs-s; this value is about 60% of the initial estimate value. The disparity could be attributed to the inefficiency of the motor's nozzle, and the assumptions made. The maximum output thrust of the hybrid motor was 377 lbs, which was obtained at the instant the motor started.

The test provided useful pressure data that was used to characterize future test runs. The team tried to make adjustments to the different elements that failed to avoid making the same mistakes in latter tests.

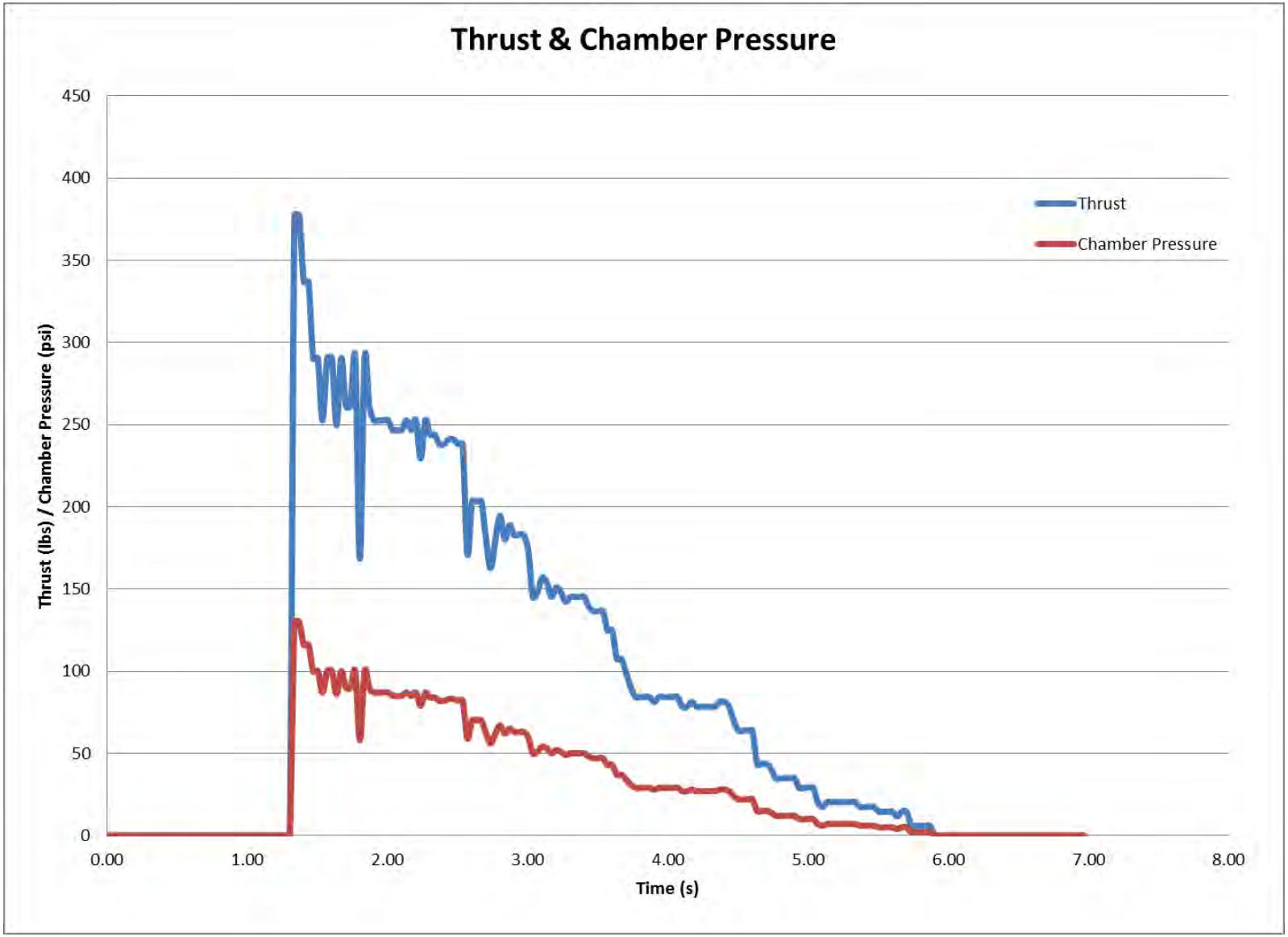

Figure 55: Thrust and Chamber Pressure Profile for Hybrid Motor

8.3. Integrated Solid Hybrid Motor Test

With a successful test of the hybrid motor prompted team HySol to go one step further and design a full solid, hybrid motor. The main difference this test would have from previous ones is that the solid grain triggering the oxidizer valve would also provide thrust. Figure 56 shows the CAD model of the motor used for this test. The nozzle of the rocket was completely redesigned to accommodate the extra propellant that would flow through it. The area of the throat is very important to determine, since it controls the chamber pressure. Table 17 shows the design values taken into consideration for this test. As with the previous test, many of the values were assumed. A throat diameter of 1.18 inches would produce a maximum pressure of 302.39 psi during the solid phase, if the correct assumptions were made. Figure 57 shows the nozzle assembly, which is composed of a PVC cap, a 0.5 phenolic insert and HTPB. The phenolic insert was added to prevent the nozzle from eroding. The HTPB layer was added to prevent nozzle erosion, and also to create a converging nozzle as it was burned by the flames. In order to expand the gases a divergent angle of 30 degrees was added to the nozzle. The 900 grams of solid propellant were spin casted into the PVC motor casing. The propellant was poured inside the casing and then spun in a lathe for approximately 5 hours. Examination of the motor after the propellant was cured showed the propellant thickness to be about 0.176 inches.

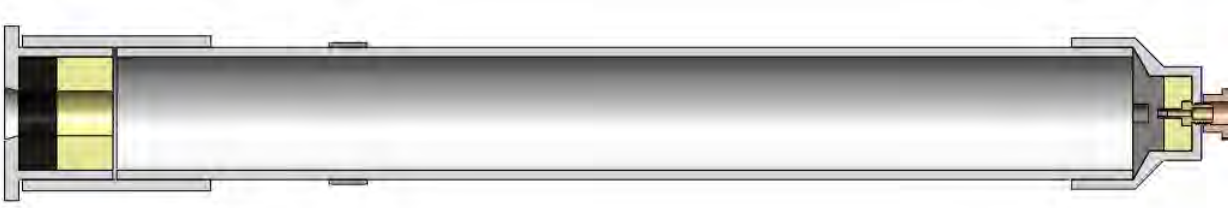

Figure 56: Solid Hybrid Motor CAD Modeling

Table 17: Design Values

I_{sp} [s]	200
Propellant Weight [lbs]	1.98
Total Impulse [lbs-s]	396.83
Regression Rate [in/s]	0.1
Solid Propellant Density [g/in^3]	23.24
Solid Propellant Volume [in^3]	38.73
PVC ID [in]	2.85
PVC length [in]	27
PVC Volume [in^3]	172.24
Core Volume [in^3]	133.52
Core Diameter [in]	2.51
Core Surface Area [in^2]	212.84
Propellant thickness [in]	0.1704
K_n	194.63
Nozzle throat Diameter [in]	1.18
Nozzle Throat Area [in^2]	1.09
P chamber	302.39
C_f	1.2

Assumed Value

Important Design Values

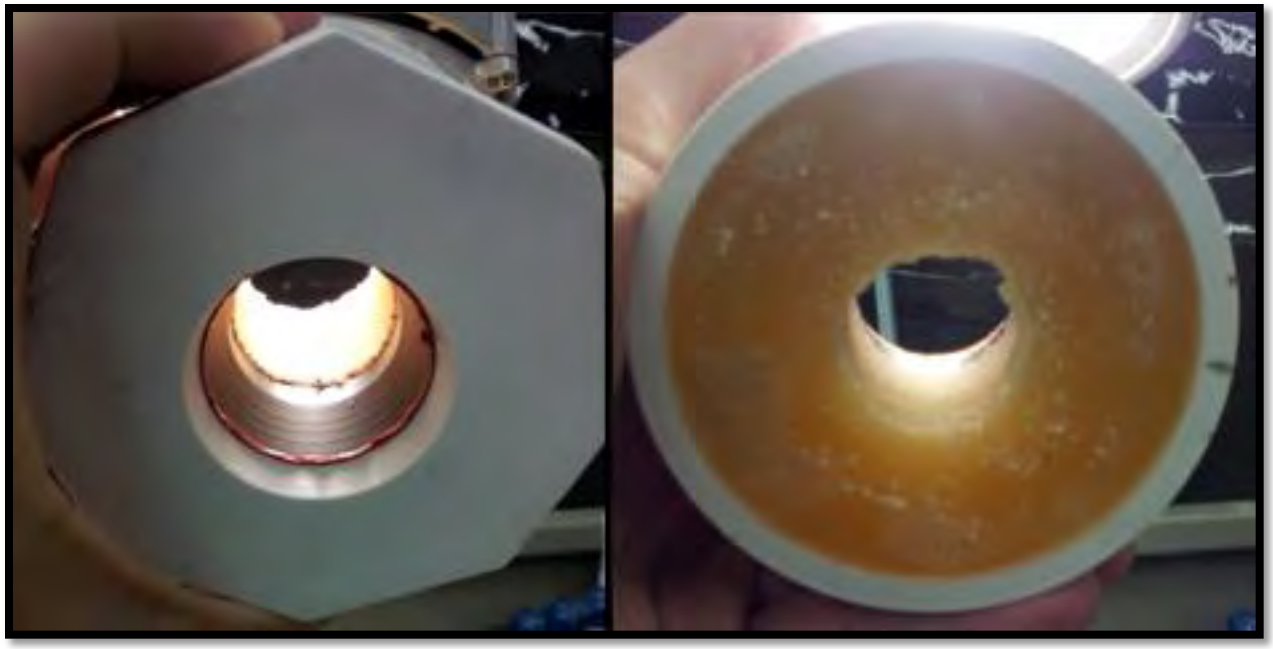

Figure 57: Nozzle Assembly

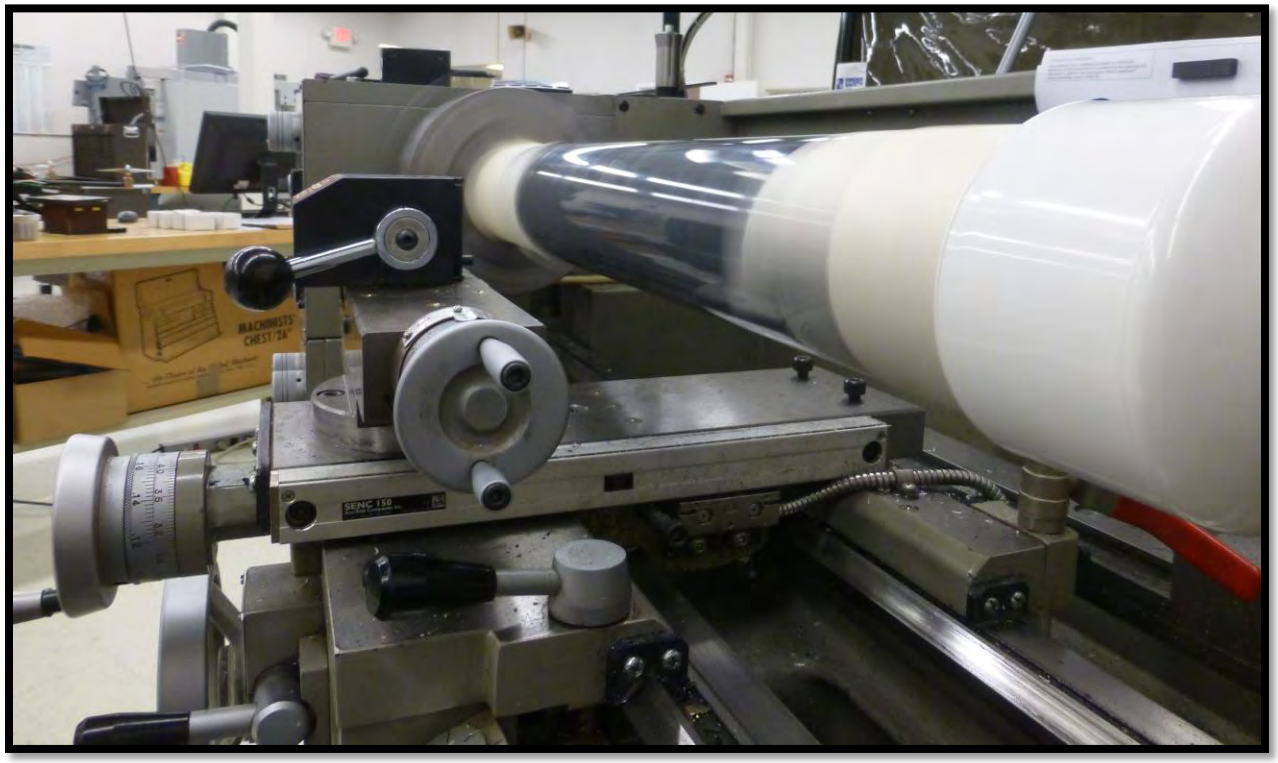

Figure 58: Solid Propellant Spin Casting

The motor failed after burning for approximately five seconds. The solid stage elevated the pressure higher than what the motor casing was designed to sustain. This scenario was taken into account, and the motor was designed to fail axially, as opposed to radially. The maximum pressure reading obtained from the pressure gage was 350 psi. Figure 59 shows the thrust and pressure profile of the solid motor before failing. The highest readings from the load cell and pressure transducer were 252 lbs and 192 psi respectively. Pressure miscalculations can be attributed to the assumptions made to calculate the throat area of the nozzle.

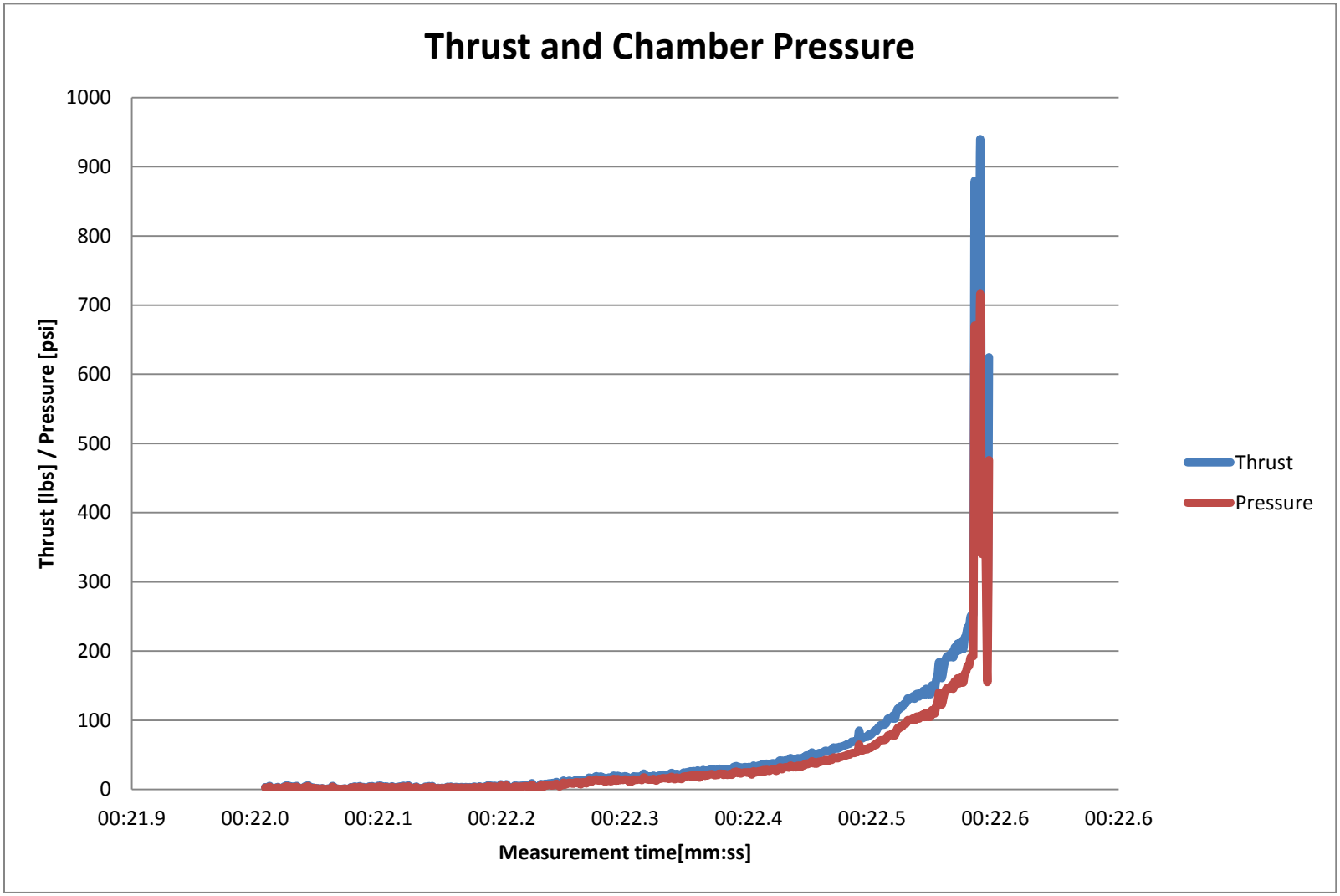

Figure 59: Thrust and Pressure Profile

9. Integrated Solid Hybrid Motor Design and Fabrication

The failure of the initial solid hybrid motor tested prompted the team to redesign it. The main concept of the motor stayed the same, however, every major structural component of the motor was reengineered (see Appendix A for detailed components). The idea behind the new concept was to be able to fly the motor after performing a successful static test. In order to accomplish the new requirement, the motor had to be reusable. An aluminum casing and bulkhead were used to avoid motor failure due to pressure. Also, a completely redesigned nozzle made out of graphite was used. The PVC tubing still played a major role in this design. It acted as the fuel for the hybrid stage. It was used as an insulator, to prevent heat soaking from the aluminum casing. Finally, it allowed the new motor to be cartridge loaded, which made the motor reusable. Figure 60 and Figure 61 show the static simulation performed in SolidWorks to the aluminum casing, no heat was added since the casing would be insulated. Figure 62 and Figure 63 show a similar simulation performed on the motor bulkhead. For this one heat transfer was considered since it was difficult to completely insulate the bulkhead. Table 18 shows the input values used to design the motor. The chamber pressure increased from approximately 300 psi to 550 psi due to the redesigned nozzle. Also, Table 19 shows the values used to calculate the length of the motor. The bulkhead and nozzle were secured using “Frankenstein” bolts. Since the graphite nozzle is very brittle an aluminum collar was used to hold the bolts and secure it. Figure 65 and Figure 66 show the manufactured bulkhead and collar. A total of 6 bolts were used to secure the two components as it can be seen in Table 20. The team designed them to hold up to 3,500 psi, in order to adjust the fuel loading when flying the motor. It is important to note that the motor was designed to fail axially and not radially.

Table 18: Hysol Motor Design Parameters

HySol Motor Design Parameters	
Isp [s]	200
Propellant Weight [lbs]	1.984
Total Impulse [lbs-sec]	396.8
Regression Rate [in/sec]	0.1
Solid Propellant Density [g/in^3]	23.24
Solid Propellant Volume [in^3]	38.73
PVC ID [in]	2.835
PVC length [in]	27
PVC Volume [in^3]	170.44
Core Volume [in^3]	131.71
Core Diameter [in]	2.492
Core Surface Area [in^2]	211.39
Propellant Web thickness [in]	0.171
Kn	193.30
Nozzle throat Diameter [in]	0.875
Nozzle Throat Area [in^2]	0.601
P chamber [psi]	550
C_f	1.2

Table 19: HySol Motor Length

Throat diameter [in]	Throat Area [in^2]	Targeted K_n
0.875	0.601	350
Port Diameter [in]	**Circumference of Port [in]**	
2.49	7.829	
Needed Length of motor for targeted K_n [in]		
26.9		

Table 20: "Frankenstein" Bolts Calculation

Bolts Calculation			
ID of the Casing [in]	3.50	Minor Diameter of Bolt [in]	0.24
Area of ID [in^2]	9.62	Area of Bolt [in^2]	0.045
Pressure [psi]	3500	Shear strength of Bolts [psi]	144000
Force due to pressure [lb]	33674	Total Area of Shear [in^2]	0.234
OD of Casing [in]	4	Min Number of Bolts	5.17
Area of OD [in^2]	12.57	Shear strength of casing [psi]	35000
Wall thickness cross section [in]	2.95	Area required for Aluminum [in^2]	0.9621
Area of wall under stress [in^2]	2.67	Number of bolts used	6
		Total area of bolt shear [in^2]	0.271

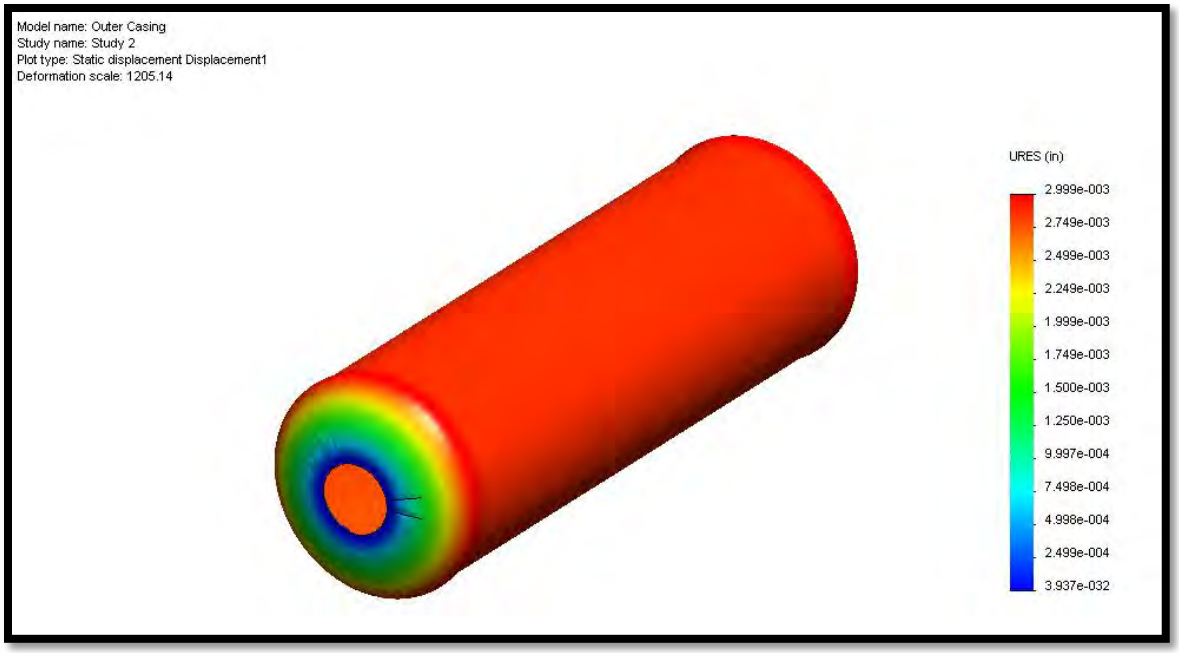

Figure 60: Outer Casing Displacement Analysis

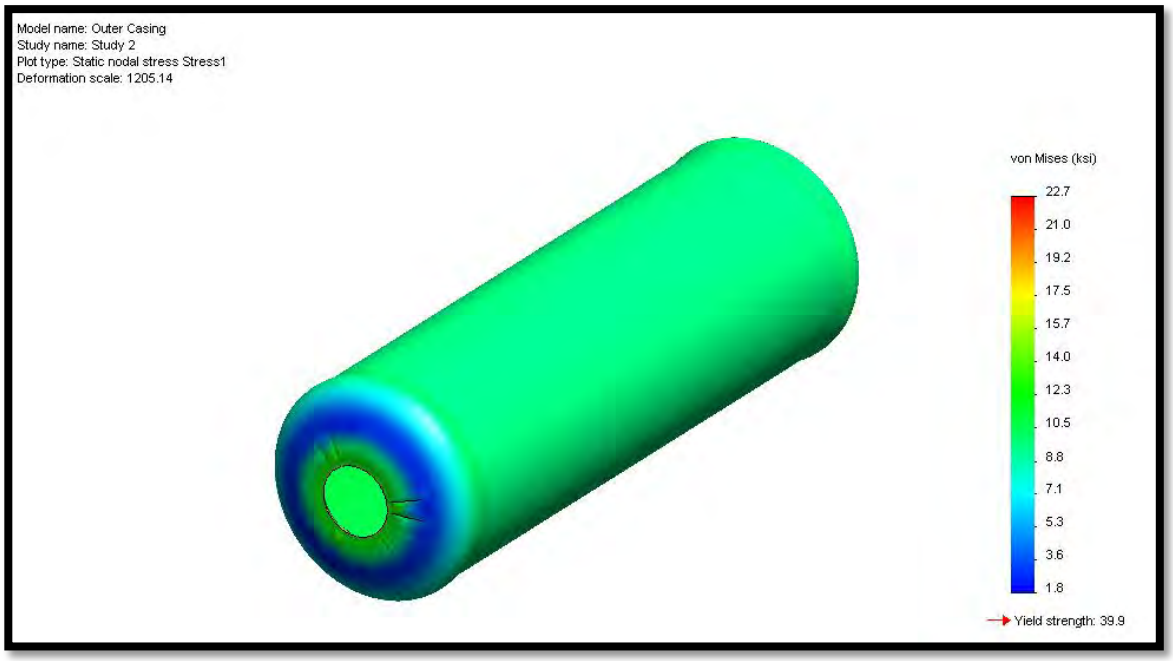

Figure 61: Outer Casing Stress Analysis

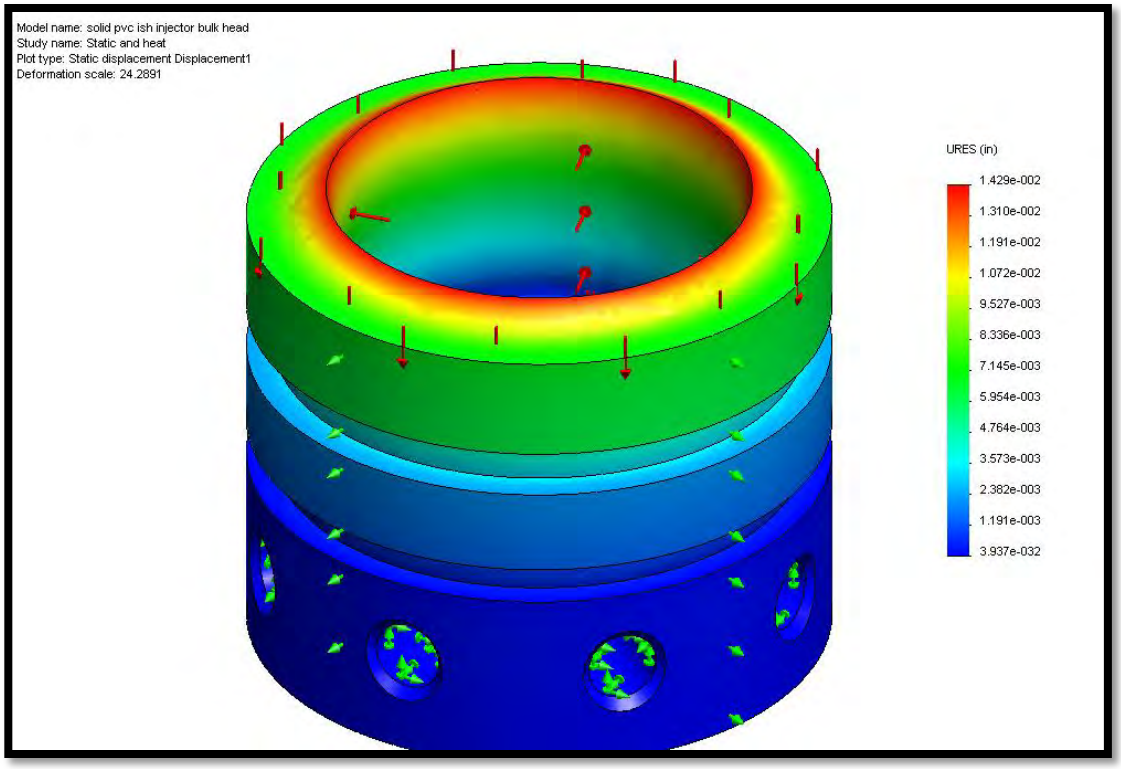

Figure 62: Bulkhead Displacement Analysis

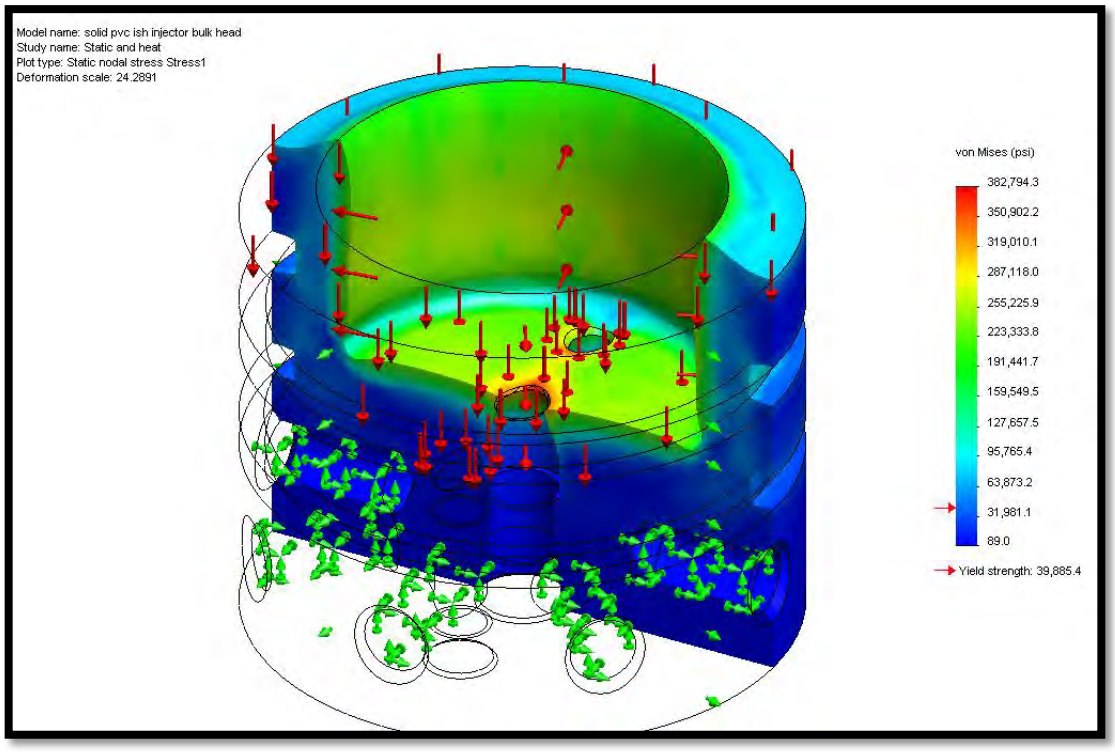

Figure 63: Bulkhead Stress Analysis

Silicone O-rings were used to seal the combustion chamber. Two of them were added to the bulkhead and the nozzle. Figure 64 shows the grooves and O-ring dimensions used. The software used for these calculations was provided by Apple-Rubber. The machining of the bulkhead and nozzle was very sensitive; the picture clearly shows that the tolerances were very small.

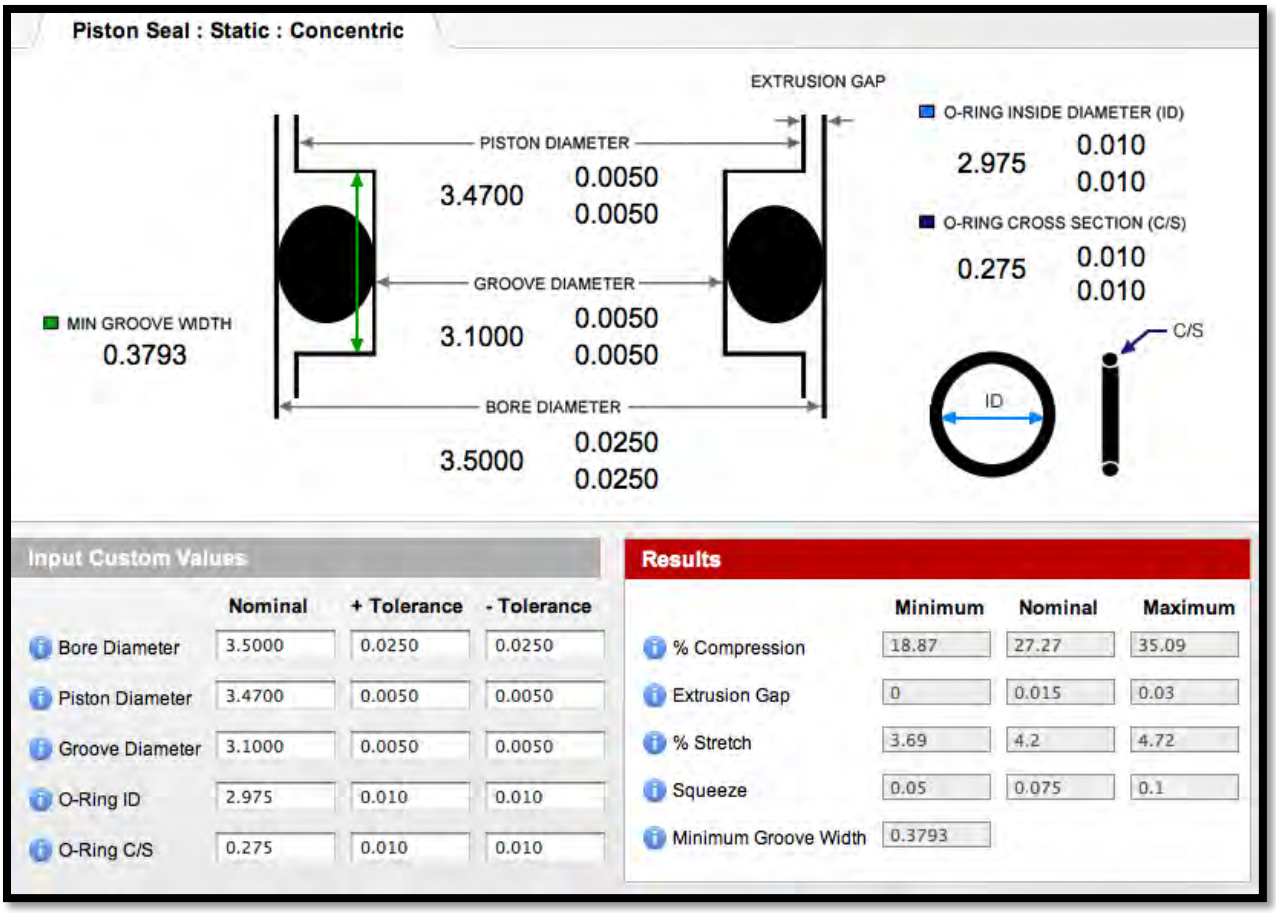

Figure 64: O-ring and Groove Dimensions

Figure 65: Aluminum Bulkhead

Figure 66: Retaining ring

Table 21 shows the motor design values used to design the nozzle. A 1,000 psi chamber pressure was used, to be able to use the same nozzle when launching the motor; this is when the team wanted the nozzle to perform more efficient. Figure 67 shows the nozzle on the lathe being manufactured. The process of manufacturing graphite was very dusty, therefore a vacuum had to be used while machining it. In Figure 68 the finished product can be appreciated. The convergent and divergent angles on the nozzle were 60° and 30° respectively. It is expected that the some erosion will be present on the throat's sharp edges after the first firing. However, this should be minimal, and should not affect the overall shape of the nozzle.

Table 21: Nozzle Design Values

Chamber Pressure	**[psi]**	1000
Ambient Pressure	**[psi]**	14.7
Expansion Ratio		6.7
Throat Diameter	**[in]**	0.875
Throat Area	**[in^2]**	0.601
Nozzle Exit Area	**[in^2]**	4.03
Nozzle Exit Diameter	**[in^2]**	2.265

Figure 67: Nozzle Manufacturing

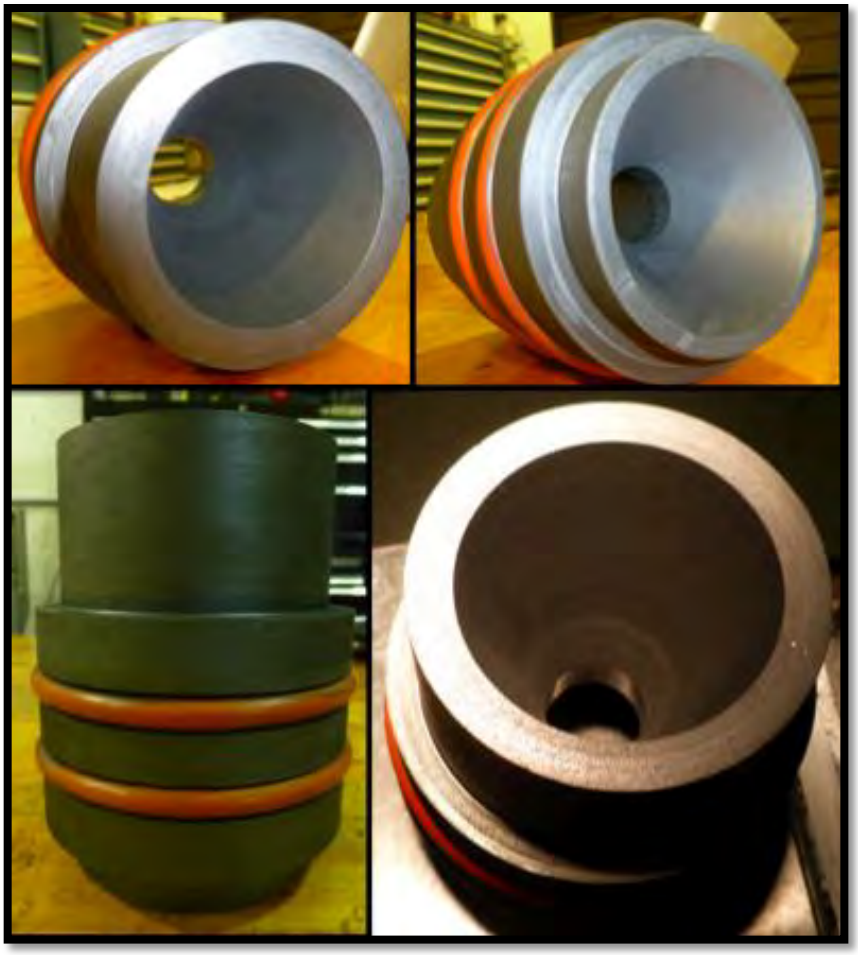

Figure 68: Graphite Nozzle

Figure 69: Rocket Motor without Outer Casing

During the initial test the team learned that the spin casting speed was a very important factor to consider. The motor had been placed at more than 500 rpm for a prolonged period of time. The centrifugal force caused the solid particles in the propellant mixture to separate from the binding agent. The final result was a layer of HPTB without any AP, and then there was another layer of

AP with some binding on it. This made the solid propellant very hard to ignite since there was little oxidizer present on the initial surface layer. Table 22 shows the necessary rotational speed to cast the motor correctly.

Table 22: Solid Fuel Casting Calculations

Solid Fuel Casting Calculations	
ID of Hybrid Motor [in]	2.835
Area of Motor [in^2]	6.312
ID of desired Solid Core [in]	2.492
Area of Core [in^2]	4.878
Length of motor [in]	26.88
Weight of propellant needed [lb]	896
Needed with waste [lb]	1030
RPM needed for casting	**237**
Velocity [in/s]	34.16652781
Radius [in]	2.75
G's	1.1
Gravity [in/s^2]	386

The team realized that spin casting at high rpms could be useful for other applications, even when it was not the desired outcome this time. Performing this process at high rpms could allow higher concentration of solids in a liquid mixture. The only downside to this process is that the binding agent on the surface would have to be scraped. More examination would be necessary to perform the setup correctly.

10. Conclusion

Power limitations have held rocketeering back in recent years. By designing a valve system, which allows the combination of both unique propellant systems, the rocket would receive sufficient power to reach our altitude goal. The team focused on designing an oxidizer injector that would automatically transition from a solid to a hybrid rocket motor. A pyrotechnic valve that performs this function was successfully designed and tested. The current design can be used with different injector configurations. The pyrotechnic technology developed could even be used in completely different injector systems. It is the group's desire to conduct further testing on the integrated solid hybrid motor to better characterize the system. Team HySol and eAc plan on building a 12-inch rocket using this new technology. This rocket motor will likely break the current amateur rocket record of 72 miles.

11. References

Bilstein, R. (1996). *Stages to Saturn a Technological History of the Apollo/Saturn launch Vehicles.* Washington D.C.: National Aeronatics and Space Administration, NASA.

Brezezinski, M. (2007). *Red Moon Rising.* New York: Henry Holt and Company.

Cadbury, D. (2006). *Space Race: The Epic Battle Between America and the Soviet Union for Dominance of Space.* New York: Harper Collins Publishers.

Cantwell, D. B. (n.d.). *Stanford Aeronautics & Astronautics.* Retrieved from Stanford University: http://aa.stanford.edu/students/media/posters2011/Ashley_Chandler.pdf

Cantwell, J. Z. (n.d.). *Stanford University*. Retrieved from Aeronautics and Astronautics: http://aa.stanford.edu/students/media/posters2012/zimmerman.pdf

Coello, A. (2002). Constraint-handling in genetic algorithms through the use of dominance-based tournament selection. *Advanced Engineering Informatics*, 193-203.

eAc. (n.d.). Retrieved from Environmental Aeroscience Corporation: http://www.hybrids.com/

Hobby Space. (n.d.). Retrieved from Advanced Rocketry: www.hobbyspace.com/Rocketry/Advanced/records.html

Hybrid Nozzle. (n.d.). Retrieved from SEDSWiki: http://wiki.seds.org/index.php?title=Hybrid_Nozzle&redirect=no

Kirk, D. R. (n.d.). *Florida Institute of Technology.* Retrieved from FIT.edu

Kline, K. S. (1998). *Patent No. 6,125,763.* United States of America.

Muncy, J. (n.d.). *Our History: Space Frontier Foundation*. Retrieved from http://spacefrontier.org/our-history/

Register, F. (n.d.). *U.S. Government Printing Office*. Retrieved from Rules and Regulations: www.gpo.gov/fdsys/pkg/FR-2008-12-04/pdf/E8-28703.pdf

Rocketry, A. (n.d.). *Hobby Space*. Retrieved from Advanced Rocketry: http://www.hobbyspace.com/Rocketry/Advanced/records.html

Rogers, C. E. (n.d.). *Nevada Aerospace Science Associates.* Retrieved from Propellant Characterization: rimworld.com

Shepherd, S. (n.d.). Fourth of July the year around. *Popular Science*, pp. 81-85.

12. Appendix

12.1. Appendix A

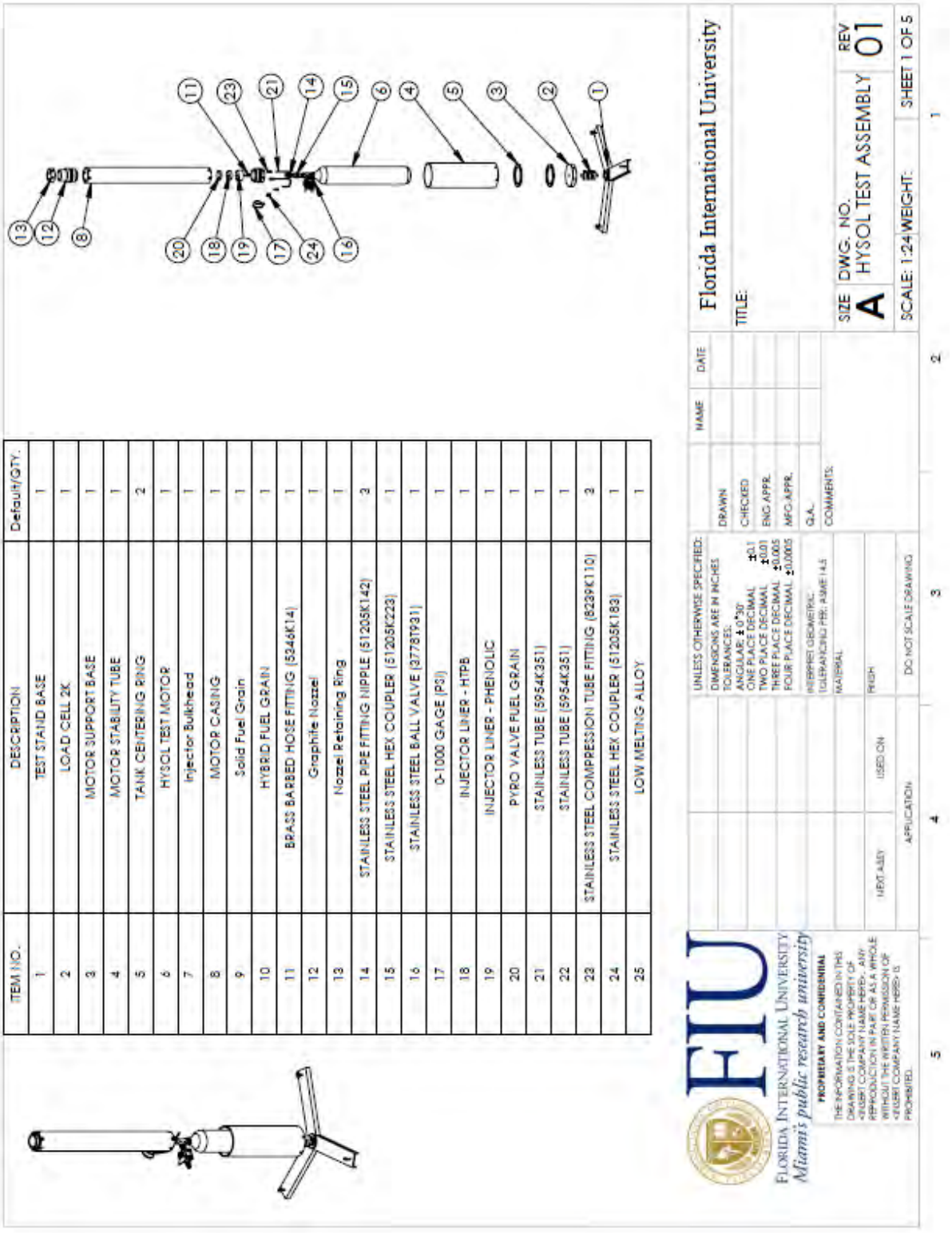

NOTES:
1. MATERIAL: ALUMMINUM 6061-T6 PER ASTM B221 - 12A
2. PARTS TO BE FREE FROM DIRT, OIL AND DEBTIS

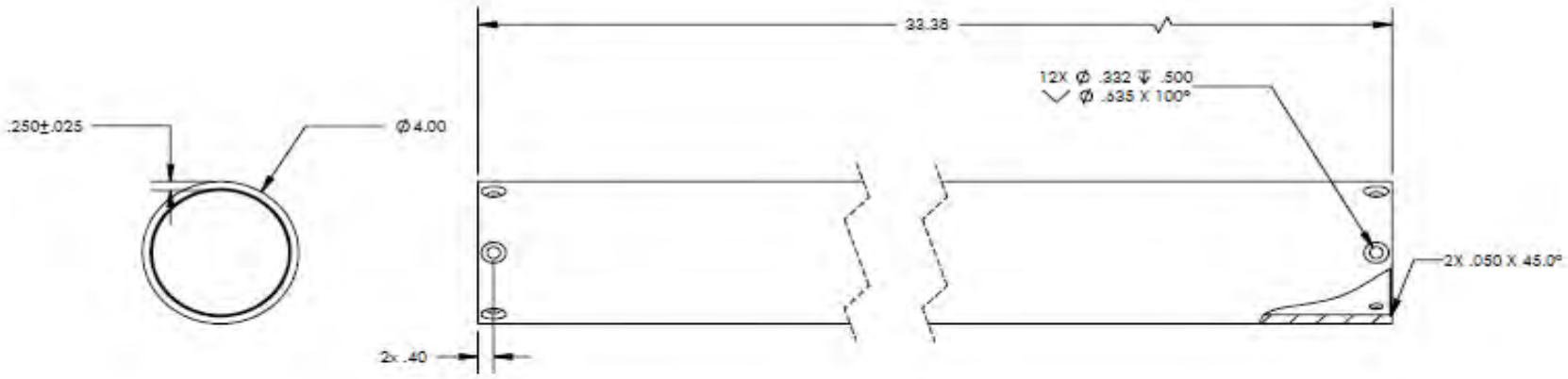

FIU
Florida International University
Miami's public research university

NEXT ASSY	USED ON	
APPLICATION		DO NOT SCALE DRAWING

UNLESS OTHERWISE SPECIFIED:
DIMENSIONS ARE IN INCHES
TOLERANCES:
ANGULAR: ± 0°30'
ONE PLACE DECIMAL ±0.1
TWO PLACE DECIMAL ±0.01
THREE PLACE DECIMAL ±0.005
FOUR PLACE DECIMAL ±0.0005
INTERPRET GEOMETRIC TOLERANCING PER: ASME Y14.5
MATERIAL
FINISH

	NAME	DATE
DRAWN		
CHECKED		
ENG APPR.		
MFG APPR.		
Q.A.		
COMMENTS:		

Florida International University

TITLE:

SIZE	DWG. NO.	REV
A	HYSOL TEST ASSEMBLY	01
SCALE: 1:4	WEIGHT:	SHEET 2 OF 5

5 4 3 2 1

NOTES:
MATERIAL: THICK-WALL DARK GRAY PVC UNTHREADED PIPE 3" PIPE SIZE, SCHEDULE 80

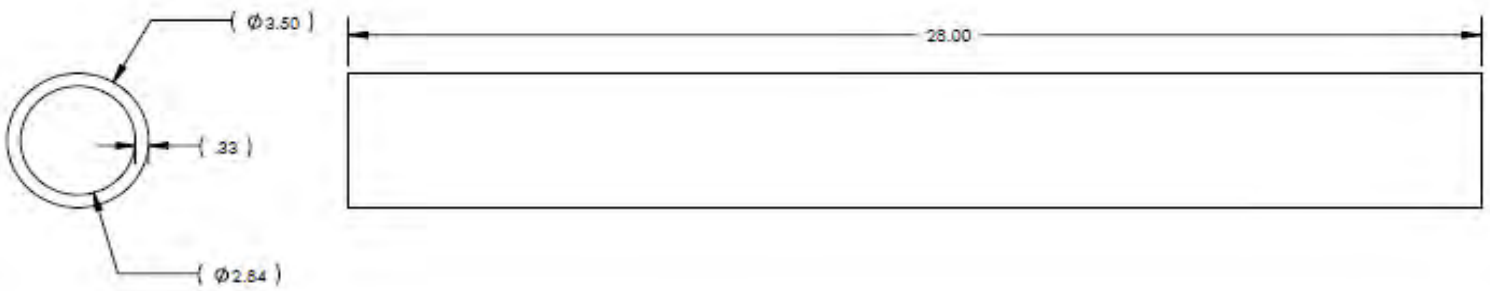

FIU
FLORIDA INTERNATIONAL UNIVERSITY
Miami's public research university

NEXT ASSY	USED ON
APPLICATION	

UNLESS OTHERWISE SPECIFIED:
DIMENSIONS ARE IN INCHES
TOLERANCES:
ANGULAR: ± 0°30'
ONE PLACE DECIMAL ±0.1
TWO PLACE DECIMAL ±0.01
THREE PLACE DECIMAL ±0.005
FOUR PLACE DECIMAL ±0.0005
INTERPRET GEOMETRIC TOLERANCING PER: ASME Y14.5
MATERIAL
FINISH
DO NOT SCALE DRAWING

	NAME	DATE
DRAWN		
CHECKED		
ENG APPR.		
MFG APPR.		
Q.A.		
COMMENTS:		

Florida International University

TITLE:

SIZE	DWG. NO.	REV
A	HYSOL TEST ASSEMBLY	01
SCALE: 1:4	WEIGHT:	SHEET 3 OF 5

5 4 3 2 1

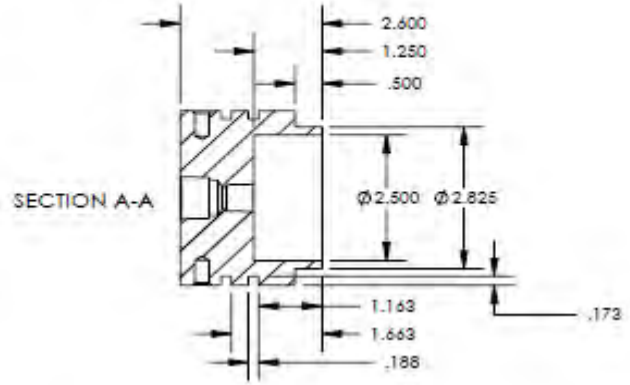

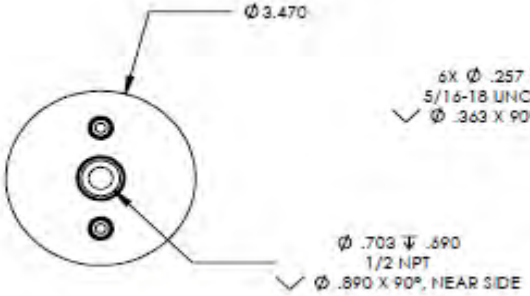

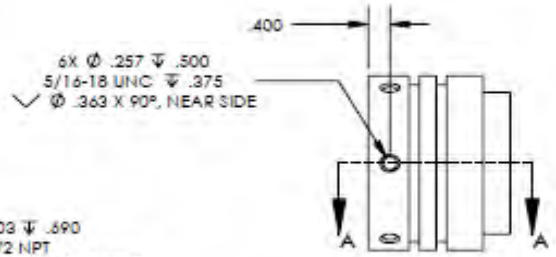

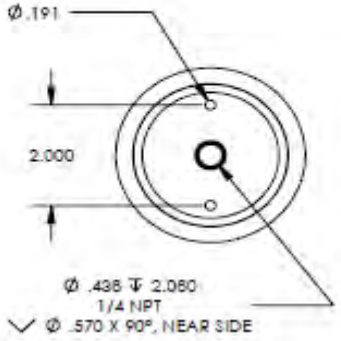

FIU
Florida International University
Miami's public research university

NEXT ASSY	USED ON
APPLICATION	

UNLESS OTHERWISE SPECIFIED:
DIMENSIONS ARE IN INCHES
TOLERANCES:
ANGULAR: ± 0°30'
ONE PLACE DECIMAL ±0.1
TWO PLACE DECIMAL ±0.01
THREE PLACE DECIMAL ±0.005
FOUR PLACE DECIMAL ±0.0005
INTERPRET GEOMETRIC TOLERANCING PER: ASME Y14.5
MATERIAL
FINISH
DO NOT SCALE DRAWING

	NAME	DATE
DRAWN		
CHECKED		
ENG APPR.		
MFG APPR.		
Q.A.		
COMMENTS:		

Florida International University

TITLE:

SIZE	DWG. NO.	REV
A	HYSOL TEST ASSEMBLY	01

SCALE: 1:3	WEIGHT:	SHEET 4 OF 5

5 4 3 2 1

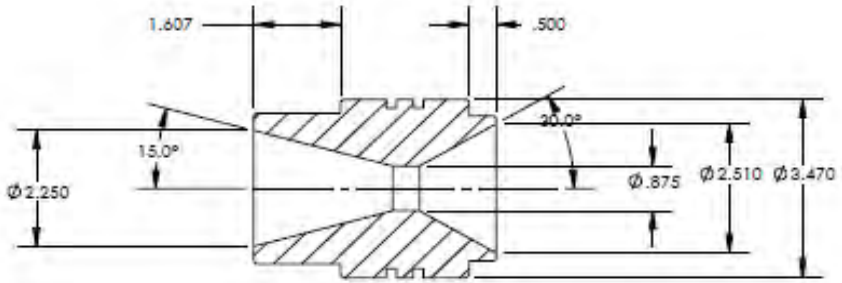

SECTION B-B

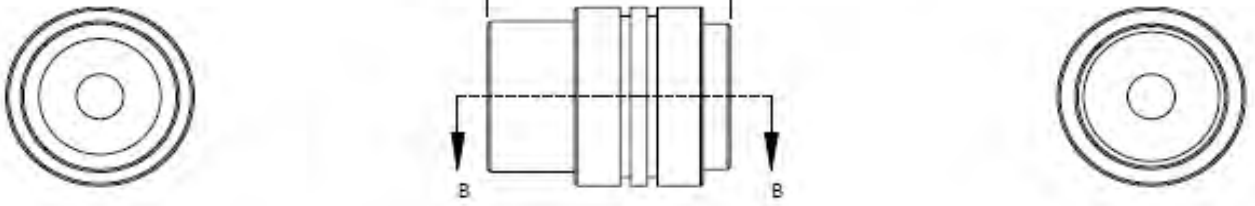

FLORIDA INTERNATIONAL UNIVERSITY
Miami's public research university

		UNLESS OTHERWISE SPECIFIED:		NAME	DATE
		DIMENSIONS ARE IN INCHES TOLERANCES: ANGULAR: ± 0°30' ONE PLACE DECIMAL ±0.1 TWO PLACE DECIMAL ±0.01 THREE PLACE DECIMAL ±0.005 FOUR PLACE DECIMAL ±0.0005	DRAWN		
			CHECKED		
			ENG APPR.		
			MFG APPR.		
		INTERPRET GEOMETRIC TOLERANCING PER: ASME Y14.5	Q.A.		
			COMMENTS:		
		MATERIAL			
NEXT ASSY	USED ON	FINISH			
APPLICATION		DO NOT SCALE DRAWING			

Florida International University

TITLE:

SIZE	DWG. NO.	REV
A	HYSOL TEST ASSEMBLY	01

SCALE: 1:3	WEIGHT:	SHEET 5 OF 5

5 4 3 2 1